XXIX Canary Islands Winter School of Astrophysics –
Applications of **Radiative Transfer** to stellar and planetary atmospheres

# Radiative transfer in the (expanding) atmospheres of early type stars, and related problems

**Jo(achim) Puls**
LMU Munich, University Observatory (USM)
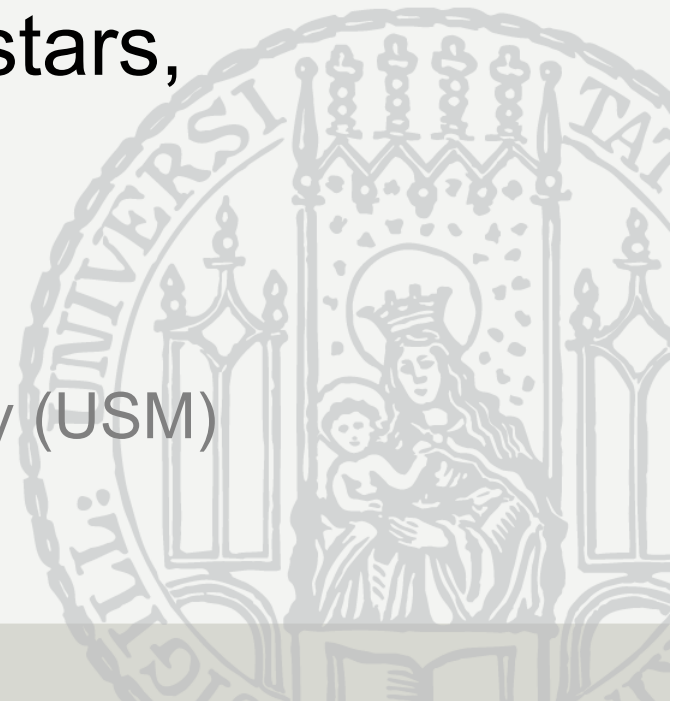
Specific text-books

Mihalas, D., "Stellar atmospheres (2nd  edition), 1975

Hubeny, I., & Mihalas, D., "Theory of stellar atmospheres", 2014

ζ Pup: SWP 27603 – Copernicus High Res

– Morton & Underhill 1977
– Howarth (p.c.)
Δt several years

$v_{max} \approx 2,500$ km/s
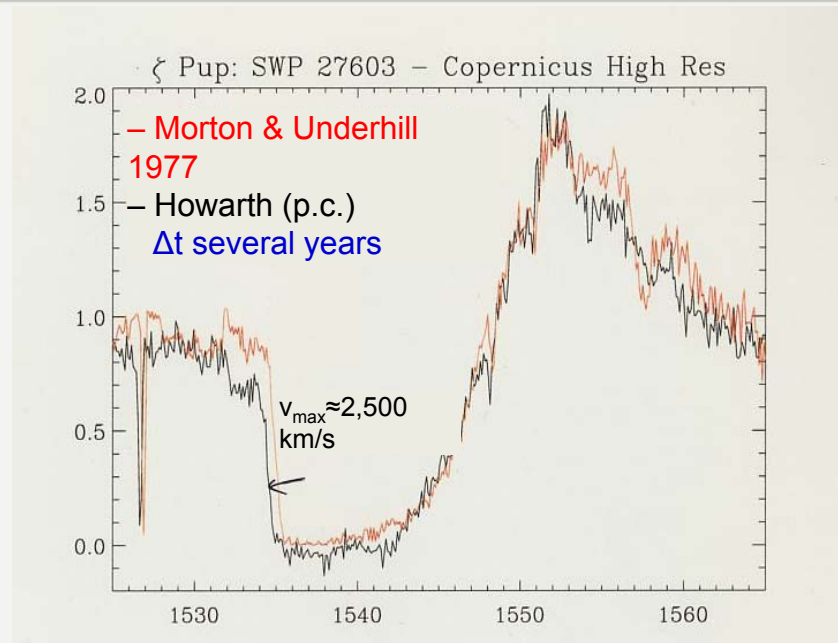
- Observational findings:
  early type star have outflows, at least quasi-stationary
- only small variability of global quantities $(\dot{M}, v_\infty)$
- $\dot{M}, v_\infty, v(r)$ have to be <u>explained</u>
- diagnostic tools have to be <u>developed</u>
- predictions have to be <u>given</u>

**Theory of expanding atmospheres**

The principle of radiatively driven winds
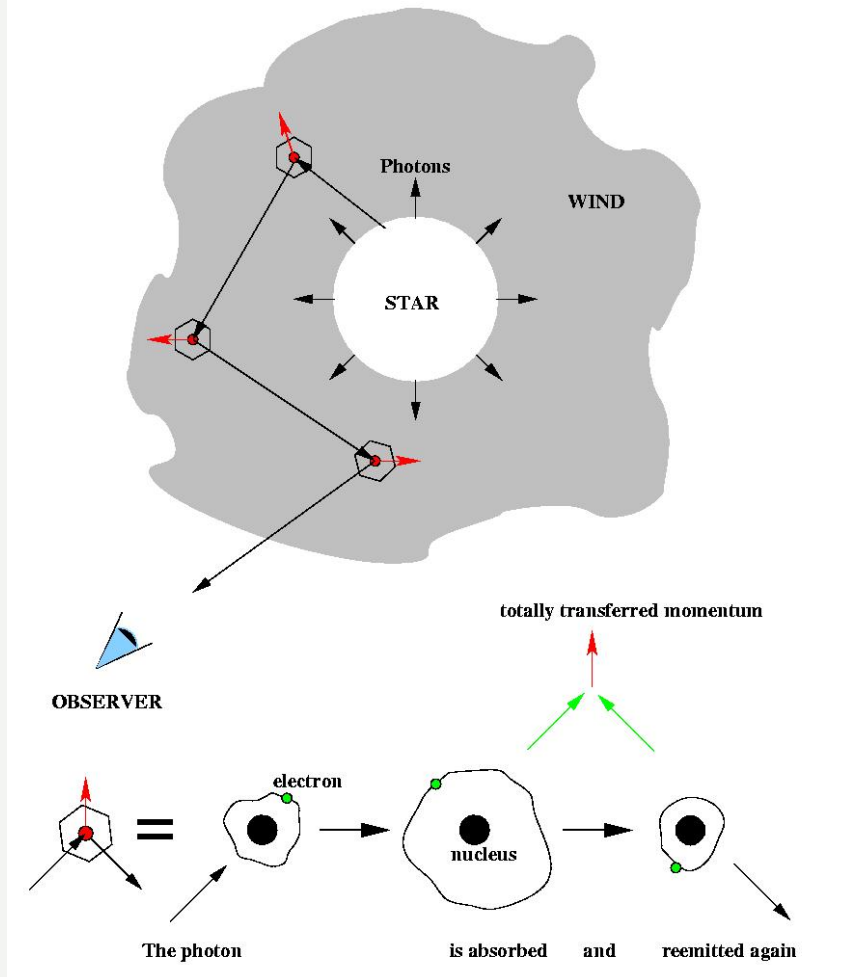
- driven by radiative line acceleration, supersonic outflows:

$$\dot{M} \approx 10^{-7}...10^{-5} \ \mathrm{M_{sun}} / \mathrm{yr}, \ \mathrm{v}_{\infty} \approx 200 \ ... \ 3,000 \ \mathrm{km/s}$$

➢ **Radiative transfer in expanding media required, both to calculate line acceleration, and to synthesize SEDs (quantitative spectroscopy)**

**Prerequisites for radiative driving**

- large number of photons *and*
- large number of lines close to flux maximum required (typically some $10^4...10^5$ lines relevant)
- … with high interaction probability (=> mass-loss dependent on metal abundances)

- dramatic impact on stellar evolution of massive stars (mass-loss rate vs. life time!)
- line driven winds important for chemical evolution of (spiral) Galaxies, in particular for starbursts
- transfer of momentum (=> might induce *star formation*), energy and nuclear-processed material to surrounding environment

**pioneering investigations** by
Lucy & Solomon, 1970
Castor, Abbott & Klein, 1975 (CAK)

**reviews** by Kudritzki & Puls, 2000
                                Puls et al. 2008

… relevant for the radiative transfer in early type stars

- **sphericity**
  (affects radiation field and density)

- **velocity fields**
  (mostly affect line-transfer, due to Dopper-shift)

light ray through atmosphere

as long as $\Delta r / R << 1$

=> plane-parallel (p-p) symmetry

spherical symmetry
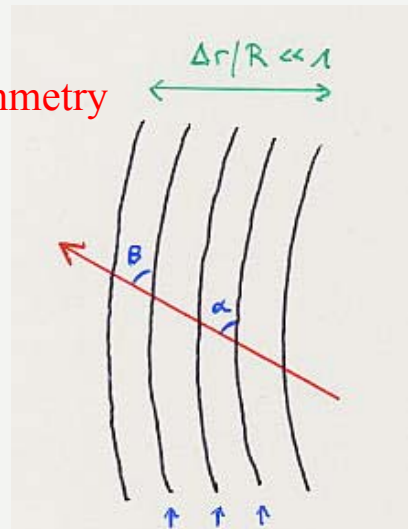


lines of constant temperature and density (isocontours)

curvature of atmosphere
insignificant for photons' path:
$\alpha = \beta$
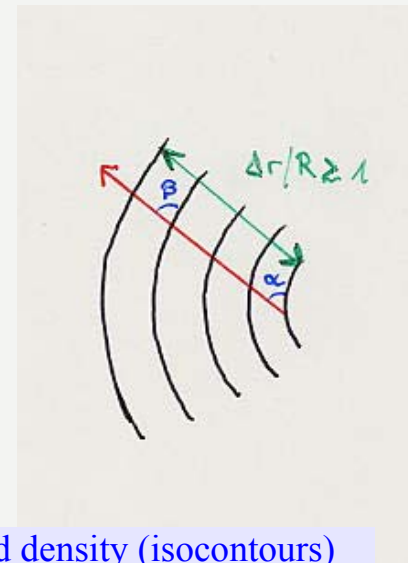
significant curvature:
$\alpha \neq \beta$

**examples**

solar photosphere / cromosphere
atmospheres of
"cool" main sequence stars
white dwarfs

solar corona
expanding envelopes (stellar winds)
of OBA stars, red giants and supergiants

### Cartesian
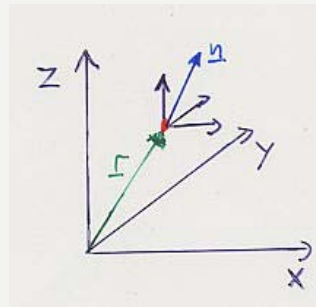
### spherical



$$\mathbf{r} = x\mathbf{e_x} + y\mathbf{e_y} + z\mathbf{e_z}$$

$$\mathbf{r} = \Theta\mathbf{e_\Theta} + \Phi\mathbf{e_\Phi} + r\mathbf{e_r}$$

$\mathbf{e_x}, \mathbf{e_y}, \mathbf{e_z}$ right-handed, orthonormal $\mathbf{e_\Theta}, \mathbf{e_\Phi}, \mathbf{e_r}$

specific intensity:

$$I(x,y,z,\mathbf{n},\nu,t) \qquad\qquad I(\Theta,\Phi,r,\mathbf{n},\nu,t)$$

important symmetries

plane-parallel

spherically symmetric

physical quantities depend
only on $z$, e.g.
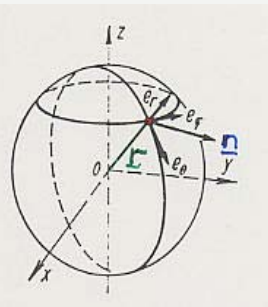
.... depend
only on $r$, e.g.

$$I(\mathbf{r},\mathbf{n},\nu,t) \to I(z,\mathbf{n},\nu,t) \qquad I(\mathbf{r},\mathbf{n},\nu,t) \to I(r,\mathbf{n},\nu,t)$$

intensity has direction $\mathbf{n}$ into $d\Omega$

$\mathbf{n}$ requires additional angles $\theta, \phi$ with respect to

$$\mathbf{e_x}, \mathbf{e_y}, \mathbf{e_z} \qquad\qquad \mathbf{e_\Theta}, \mathbf{e_\Phi}, \mathbf{e_r}$$

and

$$\theta = \sphericalangle(\mathbf{e_z}, \mathbf{n}) \qquad\qquad \theta = \sphericalangle(\mathbf{e_r}, \mathbf{n})$$

$$I_\nu(x,y,z,\theta,\phi,t) \qquad\qquad I_\nu(\Theta,\Phi,r,\theta,\phi,t)$$

p-p symmetry

spherical symmetry

independent of azimuthal direction, $\phi$

$$\to I_\nu(z,\theta,t) \qquad\qquad \to I_\nu(r,\theta,t)$$
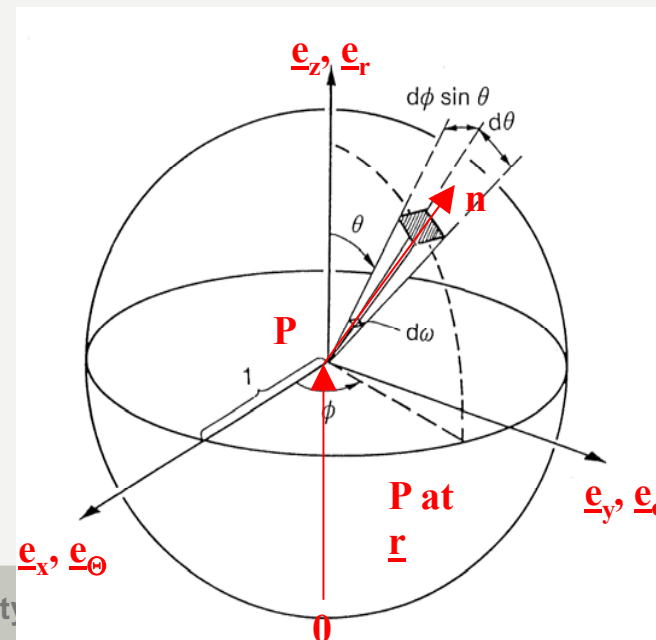
In plane-parallel atmospheres without winds (e.g., Kurucz atmospheres), hydrostatic equilibrium assumed; also in atmospheric models of early type stars with very thin winds [e.g., TLUSTY (Hubeny 1998) or DETAIL/SURFACE (Butler & Giddings 1985), see Appendix A]

$$\frac{\partial p}{\partial z} = \rho(z)\left(-g_{\text{grav}} + g_{\text{Rad}}(z)\right), \quad \text{with } g_{\text{grav}} = \frac{GM_*}{R_*^2}, \text{ assuming } \Delta z(\text{photosphere}) \ll R_*$$

Integration gives either $P_{tot}(z) = g_{\text{grav}} \cdot m$

with $P_{tot} = P_{\text{gas}} + P_{\text{rad}}$ and mass column density $m = \int_z^\infty \rho(z)\mathrm{d}z$

or, neglecting $g_{\text{rad}}$, $\rho(z) \approx \rho(z=0)\, e^{-z/H}$, with photospheric scale height $H = \frac{k_{\text{B}}T_*}{\mu m_{\text{H}} g_{\text{grav}}} = \frac{2 v_{\text{sound}}^2(T_*)}{v_{\text{esc}}^2} R_*$

$v_{\text{sound}} = \sqrt{\frac{k_{\text{B}}T}{\mu m_{\text{H}}}}$ is the isothermal speed of sound [order of few km/s], $\mu$ the mean molecular weight, and

$v_{\text{esc}} = \sqrt{\frac{2GM_*}{R_*}}$ the photospheric escape velocity [usually, order of several 100 km/s]

Alternatively (again neglecting $g_{\text{rad}}$),

$\rho(m) \approx \frac{1}{H} m$, i.e., $\log \rho = \log m - \log(H)$

Hydrodynamic description: inclusion of velocity fields

Equation of continuity:

$$\frac{\partial \rho}{\partial t} + \nabla \cdot (\rho \mathbf{v}) = 0$$

Equation of momentum
("Euler equation")

$$\frac{\partial \rho \mathbf{v}}{\partial t} + \underbrace{\nabla \cdot (\rho \mathbf{v} \otimes \mathbf{v})}_{\mathbf{v}[\nabla \cdot (\rho \mathbf{v})] + [\rho \mathbf{v} \cdot \nabla] \mathbf{v}} = -\nabla p + \rho \mathbf{g}^{\text{ext}}$$

$$\Rrightarrow$$

stationarity, i.e., $\frac{\partial}{\partial t} = 0$
and spherical symmetry,
i.e., $\nabla \cdot \mathbf{u} \rightarrow \frac{1}{r^2}\frac{\partial}{\partial r}(r^2 u_r)$

$$r^2 \rho \mathrm{v} = \text{const} = \frac{\dot{M}}{4\pi} \quad \text{(I)}$$

with $\nabla \cdot (\rho \mathbf{v}) = 0$

$$\underbrace{\rho \mathrm{v}\frac{\partial \mathrm{v}}{\partial r}}_{\substack{\text{"advection term",}\\ \text{(from inertia)}}} = -\frac{\partial p}{\partial r} + \rho g_r^{\text{ext}} \quad \text{(II)}$$

I:  Conservation of mass-flux

II: "Equation of motion"
    with gravity and radiative acceleration

$$\Rightarrow \quad \rho(r)\mathrm{v}(r)\frac{\partial \mathrm{v}}{\partial r} = -\frac{\partial p}{\partial r} + \rho(r)\left(-\frac{GM_*}{r^2} + g_{\text{Rad}}(r)\right)$$

or, to be compared with hydrostatic equilibrium

$$\frac{\partial p}{\partial r} = \rho(r)\left(-\frac{GM_*}{r^2} + g_{\text{Rad}}(r)\right) - \rho(r)\mathrm{v}(r)\frac{\partial \mathrm{v}}{\partial r}$$

hydrostatic equilibrium
in p-p symmetry:
$$\left.\right\} \frac{\partial p}{\partial z} = \rho(z)\left(-\frac{GM_*}{R_*^2} + g_{\text{Rad}}(z)\right)$$

By using $\quad p = \dfrac{k_B T}{\mu m_H} \rho = v_{sound}^2 \rho \quad$ (equation of state) , and $\dot{M} = 4\pi r^2 \rho v = \text{const}$ (for the hydrodynamic case)

the equations of motion and of hydrostatic equilibrium can be rewritten:

$$\left( v_{sound}^2 - v^2(r) \right) \frac{\partial \rho}{\partial r} = -\rho(r) \left( g_{grav}(r) - g_{Rad}(r) + \frac{dv_{sound}^2}{dr} - \frac{2v^2(r)}{r} \right) \quad \text{[hydrodynamic]}$$

$$v_{sound}^2 \frac{\partial \rho}{\partial z} = -\rho(z) \left( g_{grav}(R_*) - g_{Rad}(z) + \frac{dv_{sound}^2}{dz} \right) \quad \text{[hydrostatic, p-p]}$$

## Conclusion:

❑ for $v \ll v_{sound}$, hydrodynamic density stratification becomes ("quasi"-) hydrostatic
❑ this is reached in deeper photospheric layers, well below the sonic point, defined by $v(r_s) = v_{sound}$

Thus: p-p atmospheres using hydrostatic equilibrium give reasonable results
*even in the presence of winds* as long as investigated features (continua, lines)
are formed below the sonic point (see also slide 12)

Unified atmospheres –
density/velocity stratification
for stars with winds
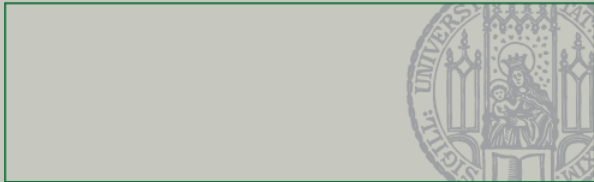
photosphere + wind = unified atmosphere (Gabler et al. 1989)

Two possibilities:
a)  stratification from theoretical wind models [Castor et al. 1975, Pauldrach et al. 1986, WM-Basic (Pauldrach et al. 2001), Appendix A]
    Disadvantage: difficult to manipulate if theory not applicable or too simplified
b)  combine quasi-hydrostatic photosphere and empirical wind structure [PHOENIX (Hauschildt 1992), CMFGEN (Hillier & Miller 1998), PoWR (Gräfener et al. 2002), FASTWIND (Puls et al. 2005), Appendix A]
    Disadvantage: transition regime ill-defined

deep layers: at first $\rho(r)$ calculated (quasi-hydrostatic, with $g_{grav}(r)$ and $g_{rad}(r)$)

$$\rightarrow \ v(r) = \frac{\dot{M}}{4\pi r^2 \rho(r)} \quad \text{for } v \ll v_{sound} \text{ (roughly: } v < 0.1 \ v_{sound})$$

outer layers: at first $v(r) = v_\infty (1 - \frac{bR_*}{r})^\beta$, "beta-velocity-law", from observations/theory (b from transition velocity)

$$\rightarrow \rho(r) = \frac{\dot{M}}{4\pi r^2 v(r)}$$

transition zone: smooth transition from deeper to outer stratification

Input/fit parameters: $\dot{M}$, $v_\infty$, $\beta$, location of transition zone
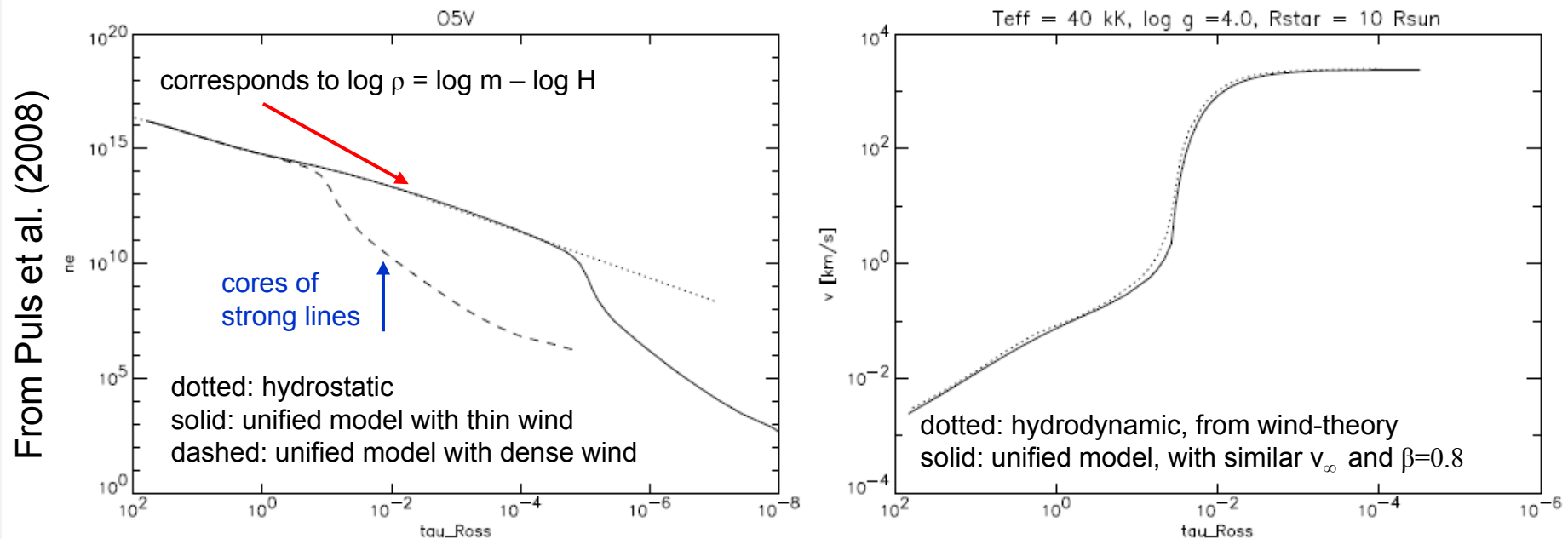
Figure 3: (Left) Electron-density as a function of the Rosseland optical depth, $\tau_{\mathrm{Ross}}$, for different atmospheric models of an O5-dwarf. Dotted: hydrostatic model atmosphere; solid, dashed: unified model with a thin and a moderately dense wind, respectively. In case of the denser wind, the cores of optical lines ($\tau_{\mathrm{Ross}} \approx 10^{-1} - 10^{-2}$) are formed at significantly different densities than in the hydrostatic model, whereas the unified, thin-wind model and the hydrostatic one would lead to similar results.

Figure 4: (Right) Velocity fields in unified models of an O-star with a thin wind. Dotted: hydrodynamic solution; solid: analytical velocity law        with similar terminal velocity and $\beta = 0.8$

NOTE: at same τ or m, wind-density (for $v \geq v_{sound}$ ) lower than if in hydrostatic equilibrium

- ❑ Unified models required if $\tau_{Ross} \geq 10^{-2}$ at transition between photosphere and wind (roughly at $0.1 * v_{sound}$)

- ❑ **rule of thumb** using a typical velocity law ($\beta=1$)

$$\dot{M}_{max} = \dot{M}(\tau_{Ross} = 10^{-2} \text{ at } 0.1 \text{ v}_{sound}) \approx 6 \cdot 10^{-8} M_\odot yr^{-1} \cdot \frac{R_*}{10 R_\odot} \cdot \frac{v_\infty}{1000 kms^{-1}}$$

- ❑ if $\dot{M}(\text{actual}) < \dot{M}_{max}$ for considered object,

   then (most) diagnostic features formed in quasi-hydrostatic part of atmosphere

- → plane-parallel, hydrostatic models possible for **optical** spectroscopy of late O-dwarfs and B-stars up to luminosity classes II (early subtypes) or Ib (mid/late subtypes)

- ❑ **check required!**

specific intensity and moments similarly defined if $z \rightarrow r$

$I(z,\mu) \rightarrow I(r,\mu)$ with $\mu=\cos\theta$ and $\theta=\sphericalangle(\mathbf{e_r}, \mathbf{n})$ [in the following, $\nu$- and $t$-dependence suppressed]

from symmetry about azimuthal direction:

$$n^{th} \text{ moment} = \frac{1}{2}\int_{-1}^{+1} I(r,\mu)\mu^n d\mu, \quad \text{as in p-p case when } z \rightarrow r; \; n=0,1,2 \rightarrow J(r), H(r), K(r)$$

flux(-density) $\mathscr{F} = \begin{pmatrix} 0 \\ 0 \\ 4\pi H \end{pmatrix}$ : only r-component different from zero, propto Eddington-flux

radiation stress tensor $\mathbf{P}$: only diagonal elements different from zero

only difference refers to divergence of radiation stress tensor, $\nabla \cdot \mathbf{P}$

in pp-symmetry, only z-component different from zero, and

$$(\nabla \cdot \mathbf{P})_z = \frac{\partial p_R}{\partial z} \text{ with } p_R \text{ (radiation pressure scalar)} = \frac{4\pi}{c}K(z)$$

in spherical symmetry, only r-component different from zero, and

$$(\nabla \cdot \mathbf{P})_r = \frac{\partial p_R}{\partial r} + \frac{3p_R - u}{r} \text{ with } u \text{ (radiation energy density)} = \frac{4\pi}{c}J(r)$$

assume:

envelope optically thin $\rightarrow I_\nu = $ const

radiation field leaving photosphere isotropic: $I_\nu^{+, \text{phot}}(\mu) = $ const $= I_\nu^+(R_*)$

$$\Rightarrow n^{\text{th}} \text{ moment } = \frac{1}{2}\int_{-1}^{+1} I_\nu(\mu)\mu^n d\mu \rightarrow \frac{1}{2}\int_{\mu_*}^{+1} I_\nu^+(R_*)\mu^n d\mu = \frac{1}{2}I_\nu^+(R_*)\frac{\left(1-\mu_*^{n+1}\right)}{n+1}$$

e.g., $J_\nu(0^{\text{th}} \text{ moment}) \approx W I_\nu^+(R_*)$ with $W$ "dilution factor,

$$W = \frac{1}{2}(1-\mu_*) \quad \text{and} \quad \mu_* = \sqrt{1-\left(\frac{R_*}{r}\right)^2} \quad \text{(cone angle subtended by stellar disk, } \sin\theta_* = \frac{R_*}{r})$$

Now, for $r \gg R_*, \quad \mu_*^{n+1} \rightarrow \left(1 - \frac{n+1}{2}\left(\frac{R_*}{r}\right)^2\right)$, and any moment

$$J_\nu = H_\nu = K_\nu = .... \rightarrow \quad \frac{1}{4}I_\nu^+(R_*)\left(\frac{R_*}{r}\right)^2$$

in other words, all Eddingfactors (ratios of moments) $\rightarrow 1$ for $r \gg R_*$

This is specific for (spherical) envelopes at large distances from the star,
and different from corresponding plane-parallel results
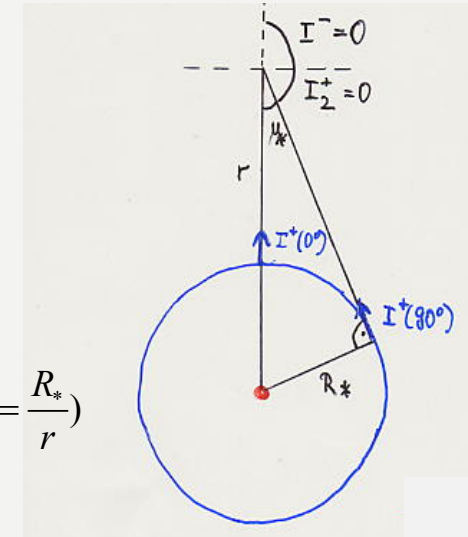
general case:

$$\left(\frac{1}{c}\frac{\partial}{\partial t} + \mathbf{n}\cdot\nabla\right)I_\nu(\mathbf{r},\mathbf{n},t) = \eta_\nu(\mathbf{r},\mathbf{n},t) - \chi_\nu(\mathbf{r},\mathbf{n},t)I_\nu(\mathbf{r},\mathbf{n},t), \qquad \text{with } \mathbf{n}\cdot\nabla \text{ directional derivative } \triangleq \frac{d}{ds}$$

plane-parallel, stationary:

$$\mathbf{n}\cdot\nabla \Rightarrow \mu\frac{d}{dz} \quad \text{(actual path is longer than height difference, } ds = dz/\mu):$$

$$\mu\frac{d}{dz}I_\nu(z,\mu) = \eta_\nu(z,\mu) - \chi_\nu(z,\mu)I_\nu(z,\mu)$$
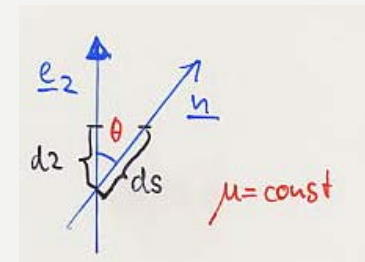


spherically symmetric, stationary ($\mu$ no longer constant along direction $\mathbf{n}$):

$$\mathbf{n}\cdot\nabla \Rightarrow \mu\frac{\partial}{\partial r} + \frac{(1-\mu^2)}{r}\frac{\partial}{\partial\mu} \quad \text{(can be shown by using a "p-z geometry", see below)}$$

$$\left(\mu\frac{\partial}{\partial r} + \frac{(1-\mu^2)}{r}\frac{\partial}{\partial\mu}\right)I_\nu(r,\mu) = \eta_\nu(r,\mu) - \chi_\nu(r,\mu)I_\nu(r,\mu)$$
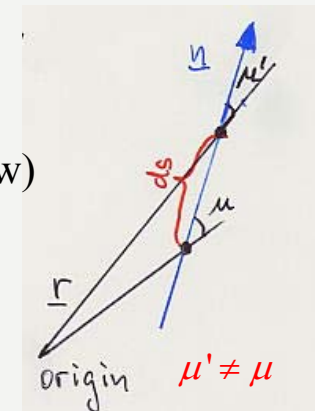
general case, 0$^{\text{th}}$ moment

$$\frac{4\pi}{c}\frac{\partial}{\partial t}J_\nu + \nabla\cdot\mathscr{F}_\nu = \oint(\eta_\nu - \chi_\nu I_\nu)\mathrm{d}\Omega$$

plane-parallel, stationary and static

$$\frac{\mathrm{d}H_\nu}{\mathrm{d}z} = \eta_\nu - \chi_\nu J_\nu$$

spherically symmetric, stationary and (quasi-)static

[no/negligible Dopplershifts $\Rightarrow$ no winds or continuum problems(except for edges)

Otherwise, opacities become angle-dependent (Doppler-shifts), and cannot be put in front of the integrals]

$$\frac{1}{r^2}\frac{\partial(r^2 H_\nu)}{\partial r} = \eta_\nu - \chi_\nu J_\nu$$

general case, 1$^{\text{st}}$ moment

$$\frac{1}{c^2}\frac{\partial}{\partial t}\mathscr{F} + \nabla\cdot\mathbf{P}_\nu = \frac{1}{c}\oint(\eta_\nu - \chi_\nu I_\nu)\mathbf{n}\mathrm{d}\Omega$$

$$\frac{\mathrm{d}K_\nu}{\mathrm{d}z} = -\chi_\nu H_\nu$$

$$\frac{\partial K_\nu}{\partial r} + \frac{3K_\nu - J_\nu}{r} = -\chi_\nu H_\nu$$

when frequency integrated, = 0, if ONLY radiation energy transported: radiative equilibrium, flux conservation

when frequency integrated, = -$f_{\text{rad}}$

NOTE: the following method (based on Hummer & Rybicki 1971) works
ONLY for spherically symmetric problems and no Doppler-shifts!
a) define p-rays (impact-parameter) tangential to each discrete radial shell
b) augment those by a bunch of (equidistant) p-rays resolving the core
c) use only the forward hemisphere, i.e.,

$$z_{di} = \sqrt{r_d^2 - p_i^2} \quad \text{and } z_{di} > 0$$

$\Rightarrow$ all points $z_{di}, i = 1, NP$, are located on the same $r_d$-shell, i.e., have the same
physical parameters such as emissivities, opacities, velocities, ...
(due to spherical symmetry, and neglect of Doppler-shifts)

Now one solves the RTE along each p-ray: from first principles,

$$\pm \frac{dI_v^\pm(z, p_i)}{dz} = \eta_v(r) - \chi_v(r)I_v^\pm(z, p_i) \quad \text{(with '+' for } \mu > 0 \text{ and '−' for } \mu < 0)$$

using appropriate boundary conditions (core vs. non-core rays),
and standard methods (finite differences etc.)



After being calculated, $I_v^\pm(z_{di}(r_d), p_i)$, $i = 1, NP$, samples the specific intensity at the same radius, $\vec{r_d}$, but at different angles,

$$\pm \mu_{di} = \frac{z_{di}}{r_d}, \quad \text{starting at } |\mu_{di}| = 1 \text{ for } i = 1 \text{ and } d = 1, NZ \text{ (central ray, } p_i = 0) \text{ to } \mu_{di} = 0 \text{ (tangent ray, where } p_i = r_d \text{ and thus } z_{di} = 0).$$

In other words, along individual $r_d$-shells, the specific intensities $I_v^\pm(r_d, \mu) = I_v^\pm(z_d, \mu)$ are sampled for all relevant $\mu$,
and corresponding moments can be calculated by integration.
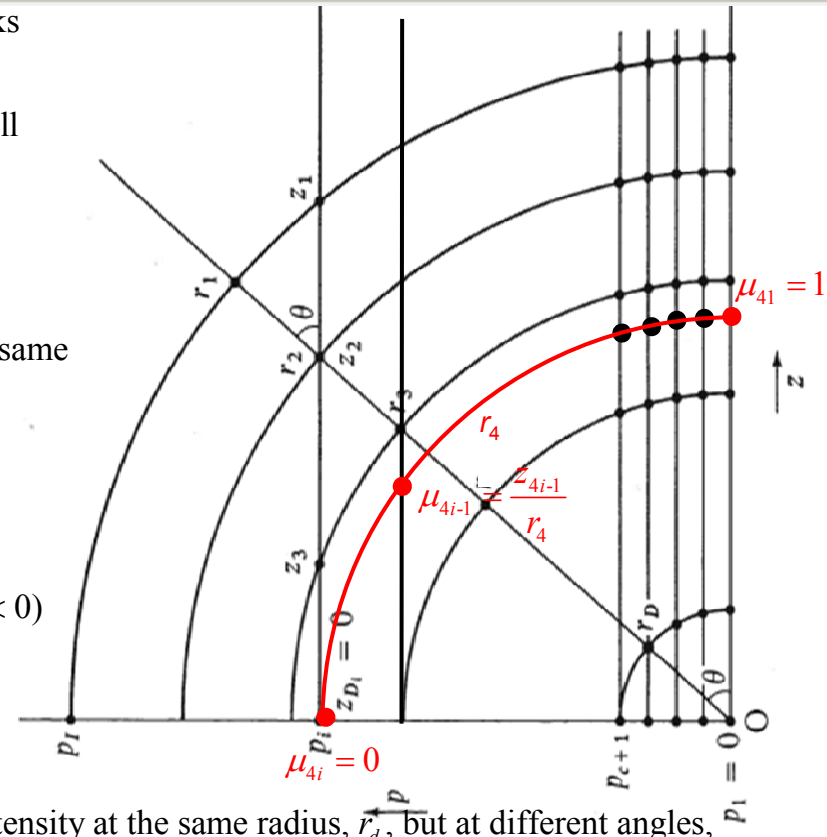
In fact, the RTE is not solved for $I_\nu^\pm$ seperately, but for a linear combination of $I_\nu^+$ and $I_\nu^-$,

using the so-called Feautrier-variables $u_\nu$ and $v_\nu$, which allows to construct a 2nd order scheme

as in the plane-parallel case: higher accuracy, diffusion limit can be easily represented

$$u_\nu(z,p) = \frac{1}{2}(I_\nu^+(z,p) + I_\nu^-(z,p)) \qquad \text{mean intensity like}$$

$$v_\nu(z,p) = \frac{1}{2}(I_\nu^+(z,p) - I_\nu^-(z,p)) \qquad \text{flux like}$$

$$\Rightarrow \frac{\partial v_\nu}{\partial z} = \chi_\nu(S_\nu - u_\nu), \quad \frac{\partial u_\nu}{dz} = -\chi_\nu v_\nu$$

$$\Rightarrow \frac{\partial^2 u_\nu}{\partial \tau_\nu^2} = u_\nu - S_\nu \quad \text{(2nd order, with } d\tau_\nu = -\chi_\nu dz)$$

... and corresponding boundary conditions

inner boundary: for core rays, first order, using the diffusion approximation; for non-core rays, 2nd order, using symmetry arguments

outer boundary: either $I_\nu^-(z_{max}, p) = 0$, or higher order for optically thick conditions (e.g., shortward of HeII Lyman edge)

Formal solution for $I_\nu(\mu)$ (or $u_\nu(\mu)$ and $v_\nu(\mu)$) and corresponding angle-averaged quantities (moments) affected by inaccuracies,

due to specific way of discretization, but ratios of moments much more precise (errors cancel to a large part)

Thus: variable Eddington-factor method

solve the moments equations (only radius-dependent), and use Eddington-factors from formal solution

to close the relations. Ensures high accuracy (since direct solution for angle-averaged quantities, and 2nd order scheme),

whilst Eddington-factors (from the formal solution) quickly stablilize in the course of global iterations.

Additional advantage: when using moments equations, optimum diagonal accelerated lambda-operator (see Chap. 4)

can be easily calculated.

Using the $0^{\text{th}}$ and $1^{\text{st}}$ moment of the RTE (see slide 16) and $f_\nu = K_\nu / J_\nu$, we obtain

$$\frac{\partial(r^2 H_\nu)}{\partial \tau_\nu} = r^2 (J_\nu - S_\nu)$$

$$\frac{\partial(f_\nu J_\nu)}{\partial \tau_\nu} - \frac{(3 f_\nu - 1) J_\nu}{\chi_\nu r} = H_\nu$$

Introducing a "sphericity factor" $q_\nu$ via $\ln(r^2 q_\nu) = \int_{r_{\text{core}}}^{r} \left[ (3 f_\nu - 1)/(r' f_\nu) \right] dr' + \ln(r_{\text{core}}^2)$, the 2nd equation becomes

$$\frac{\partial(f_\nu q_\nu r^2 J_\nu)}{\partial \tau_\nu} = q_\nu r^2 H_\nu, \text{ and can be combined with the first one to yield a 2nd order scheme for } r^2 J_\nu$$

$$\frac{\partial^2 (f_\nu q_\nu r^2 J_\nu)}{\partial X_\nu^2} = \frac{1}{q_\nu} r^2 (J_\nu - S_\nu) \quad \text{with } dX_\nu = q_\nu d\tau_\nu \quad [\text{for comp.: in p-p, } \frac{\partial^2 (f_\nu J_\nu)}{\partial \tau_\nu^2} = (J_\nu - S_\nu), \text{ limit for } q_\nu \to 1 \text{ and } r^2 \to R_*^2]$$

**Problem** (to be detailed below)
When standard (observers's frame) RT-methods applied,
very high resolution in radial grid ($\Delta v = O(v_{th}/3)$) required
(for specific methods, also very high resolution in μ required).
E.g., for $v_\infty$=2000 km/s, and $v_{th}(O)$=8km/s, N=750 radial grid points!
(problem becomes mitigated, when large "micro-turbulence" of order 100 km/s – due to inhomogeneous wind structure – considered)


NOTE as well:
Use only RTE (maybe cast into "Rybicki form" if separation into scattering and thermal part possible), but do NOT use moments equations as before, since only general formulation (top of slide 16) valid if opacities strongly μ-dependent (due to Doppler-shifts)


In the following, we mostly consider the pure line case (except when stated differently), assuming that the continuum is optically thin (not so wrong for "normal" OB-star winds, but invalid, e.g., for WR-stars with much larger mass-loss rates).


Moreover, we assume pure Doppler-broadening, which captures the essential contribution when calculating occupation numbers etc. ($\rightarrow$ scattering integral $\bar{J}$).
For the calculation of emergent profiles, other broadening functions might/should be used if necessary (e.g., Stark- and Voigt-profiles)

$$\chi_\nu(r) = \bar{\chi}_L(r)\,\phi(\nu,r) \quad \text{with} \quad \phi(\nu,r) = \frac{1}{\Delta\nu_D(r)\sqrt{\pi}}\exp\left[-\left(\frac{\nu-\tilde{\nu}}{\Delta\nu_D(r)}\right)^2\right] \quad \text{and} \quad \Delta\nu_D(r) = \frac{\tilde{\nu}\mathrm{v}_{th}(r)}{c} \quad \text{for a Doppler profile,}$$

$$\bar{\chi}_L(r) = \frac{\pi e^2}{m_e c}f_{lu}(n_l - n_u\frac{g_l}{g_u}), \quad \tilde{\nu} \text{ is the line-center frequency, and } \mathrm{v}_{th}(r) \text{ includes any micro-turbulence if present.}$$

NOTE: $\left[\bar{\chi}_L\right] = \mathrm{cm}^{-1}\mathrm{s}^{-1}$ and not $\mathrm{cm}^{-1}$, $\left[\phi\right] = \mathrm{s}$

Due to the apparent Doppler-shifts (material is moving w.r.t. stellar rest-frame), absorbing/emitting ions "see" the radiation field at corresponding comoving frame (CMF) frequencies, and absorb/emit photons according to

$$\nu_{CMF} \approx \nu - \frac{\tilde{\nu}}{c}\mathbf{n}\cdot\mathbf{v}(\mathbf{r}), \quad \text{when the observer's frame frequency is } \nu, \quad \text{and } \mathbf{n}\cdot\mathbf{v}(\mathbf{r}) = \mu\mathrm{v}(r) \text{ in spherical symmetry.}$$

Thus, the profile function has to be evaluated at the CMF-frequency,

$$\phi(\nu_{CMF},r) = \frac{1}{\Delta\nu_D(r)\sqrt{\pi}}\exp\left[-\left(\frac{\nu-\tilde{\nu}-\mu\mathrm{v}(r)\tilde{\nu}/c}{\Delta\nu_D(r)}\right)^2\right].$$

For simplicity, in the following we assume a spatially constant thermal speed, $\mathrm{v}_{th}$, and measure frequencies in Doppler-units w.r.t. to this speed (a generalization to depth-dependent $\mathrm{v}_{th}(r)$ is provided in Appendix B.1);

$$x = \frac{\nu-\tilde{\nu}}{\Delta\nu_D} \quad \text{with} \quad \Delta\nu_D = \frac{\tilde{\nu}\mathrm{v}_{th}}{c}.$$

Then, $\dfrac{\nu-\tilde{\nu}-\mu\mathrm{v}(r)\tilde{\nu}/c}{\Delta\nu_D} = x - \mu\mathrm{v}'(r) \quad \text{with} \quad \mathrm{v}'(r) = \dfrac{\mathrm{v}(r)}{\mathrm{v}_{th}} \in (0, \dfrac{\mathrm{v}_\infty}{\mathrm{v}_{th}} \gg 1].$

In this notation,

$$\phi_\nu(x_{\mathrm{CMF}}, r) = \phi_\nu(x - \mu\mathrm{v}', r) = \frac{1}{\Delta\nu_{\mathrm{D}}\sqrt{\pi}} \exp\left[-\left(x - \mu\mathrm{v}'(r)\right)^2\right],$$

the profile function has still units "per frequency", $[\phi] = \mathrm{s}$, and is only expressed with argument $x$.

To simplify the following considerations, we include the factor $(\Delta\nu_{\mathrm{D}})^{-1}$ from above into the opacity; then the profile function has units "per Doppler-shift" (i.e., it's dimensionless and normalized w.r.t. $x$), whilst $[\,\bar{\chi}_{\mathrm{L}}(r)/\Delta\nu_{\mathrm{D}}\,] = [\mathrm{cm}^{-1}]$

$$\chi_\nu(x_{\mathrm{CMF}}, r) = \frac{\bar{\chi}_{\mathrm{L}}(r)}{\Delta\nu_{\mathrm{D}}}\, \phi(x_{\mathrm{CMF}}, r) \quad \text{with} \quad \phi(x_{\mathrm{CMF}}, r) = \frac{1}{\sqrt{\pi}} \exp\left[-\left(x - \mu\mathrm{v}'(r)\right)^2\right], \quad \text{and} \quad \frac{\bar{\chi}_{\mathrm{L}}(r)}{\Delta\nu_{\mathrm{D}}} = \frac{\bar{\chi}_{\mathrm{L}}(r)\tilde{\lambda}}{\mathrm{v}_{\mathrm{th}}};$$

Note that since $\mu\mathrm{v}'(r) \in [-\frac{\mathrm{v}_\infty}{\mathrm{v}_{\mathrm{th}}}, +\frac{\mathrm{v}_\infty}{\mathrm{v}_{\mathrm{th}}}]$, $x$ needs to vary in the same range $\left[\text{essentially}, x \in (-\infty, \infty)\right]$, and not only over a few thermal Doppler widths.

For various integrals involving Φ, see Appendix B.2

Since $\mu v'(r)$ part of argument of $\phi$, we need to know $\dfrac{d\mu v'(r)}{ds}$ along path $ds$ (remember: $\mathbf{n}\cdot\nabla = \dfrac{d}{ds}$)

To calulate this quantity, we again make use of the p-z geometry in spherical symmetry (rotate such that $z\|\mathbf{n}$)

$$\frac{d\mu v'(r)}{ds} \rightarrow \left.\frac{d\mu v'(r)}{dz}\right|_p = \mu\left.\frac{dv'}{dr}\frac{dr}{dz}\right|_p + \left.\frac{d\mu}{dz}\right|_p v' = \mu^2\frac{dv'}{dr} + (1-\mu^2)\frac{v'}{r} > 0 \quad \text{for } v' > 0 \text{ and } \frac{dv'}{dr} > 0!$$

[In contrast to slide 17, $\mu < 0$ implies here $z < 0$, i.e., for negative angles we consider the back-hemisphere]

In spherical symmetry, $\mu v'(r)$ increases monotonically along any given direction $\mathbf{n}$, as long as $v' > 0$ is monotonically increasing.

(blue edge) begin    center    end (red edge)
of **resonance zone** for $x_1 = \mu v'_1$
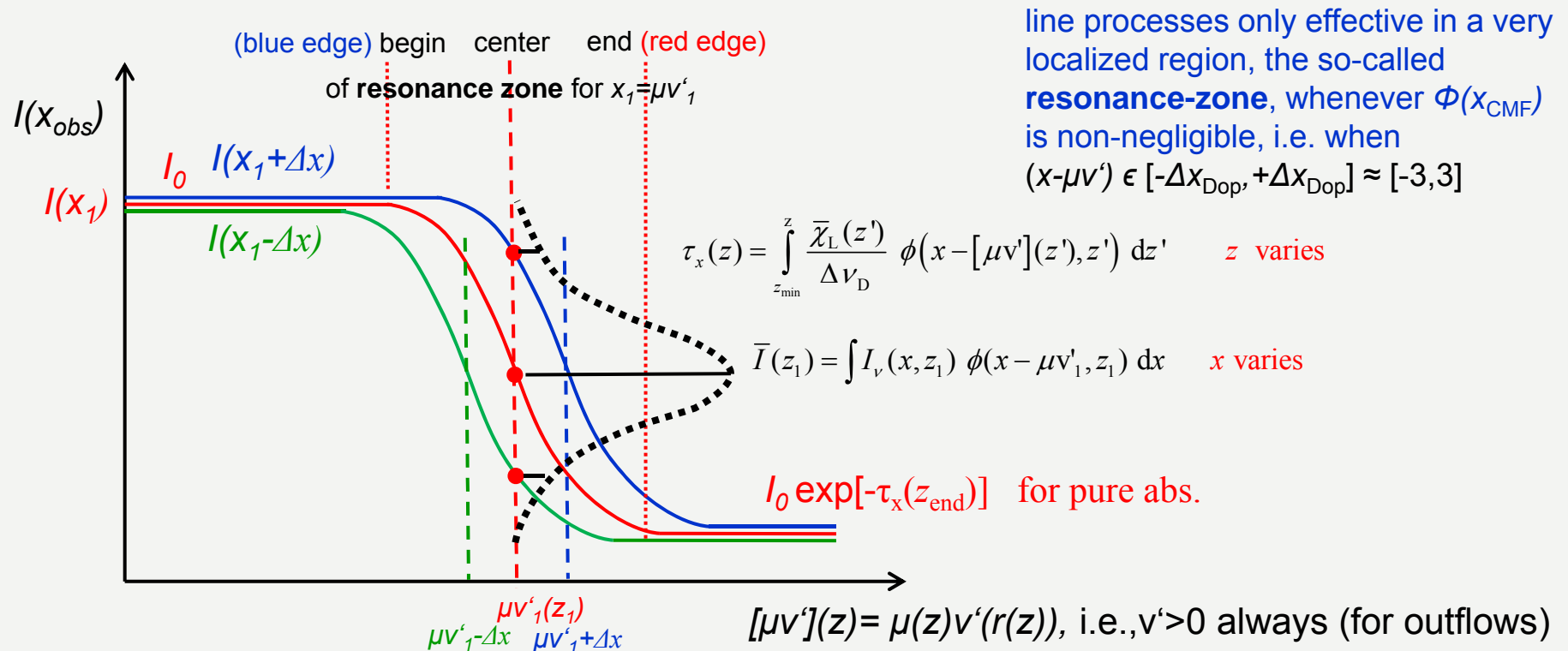
line processes only effective in a very localized region, the so-called **resonance-zone**, whenever $\Phi(x_{\text{CMF}})$ is non-negligible, i.e. when $(x-\mu v') \in [-\Delta x_{\text{Dop}}, +\Delta x_{\text{Dop}}] \approx [-3,3]$

$I(x_{obs})$

$I_0$  $I(x_1+\Delta x)$

$I(x_1)$

$I(x_1-\Delta x)$

$$\tau_x(z) = \int\limits_{z_{min}}^{z} \frac{\overline{\chi}_L(z')}{\Delta\nu_D}\, \phi\big(x-[\mu v'](z'),z'\big)\, dz' \qquad z \text{ varies}$$

$$\overline{I}(z_1) = \int I_\nu(x,z_1)\,\phi(x-\mu v'_1, z_1)\, dx \qquad x \text{ varies}$$

$I_0\exp[-\tau_x(z_{end})]$  for pure abs.

$\mu v'_1(z_1)$
$\mu v'_1-\Delta x$  $\mu v'_1+\Delta x$

$[\mu v'](z) = \mu(z)v'(r(z))$, i.e., $v' > 0$ always (for outflows)

Both freq. grid ($x$) and $\mu v'(z)$ need to be highly resolved, on scales corresponding to $v_{Dop}$.

❏ if $\mu v'(z)$-spacing too coarse: resonance zone missed or not resolved, intensity remains constant (or too large), and $\bar{I}$ becomes too large! (red, blue and green curves would become constant at $I_0$)

❏ if $x$-spacing too coarse: variation of $I(x)$ ("neighboring" resonance zones) not sufficiently sampled. (blue/green curves might be absent, and red curve not centered, if no frequency where $x-\mu v'=0$)

❏ In spherical geometry, the first point is a specific problem, since the *general spacing* has to be provided for the *radial grid* (and not for specific p-rays), and a high resolution in $v'(r)$ does not guarantee a high resolution in $\mu v'(z)$.

❏ In models using Cartesian co-ordinates ($\mu$=const along a specific ray), this leads to the condition that $\Delta\mu=\Delta x/v'_{max}$ (intricate coupling of frequency and angle!)



(blue edge) begin    center    end (red edge)
of **resonance zone** for $x_1=\mu v'_1$

$I(x_{obs})$
$I_0$    $I(x_1+\Delta x)$
$I(x_1)$
$I(x_1-\Delta x)$

$\mu v'_1(z_1)$
$\mu v'_1-\Delta x$    $\mu v'_1+\Delta x$

$$\tau_x(z) = \int_{z_{min}}^{z} \frac{\bar{\chi}_L(z')}{\Delta \nu_D} \, \phi\big(x-[\mu v'](z'),z'\big) \, dz' \qquad z \text{ varies}$$
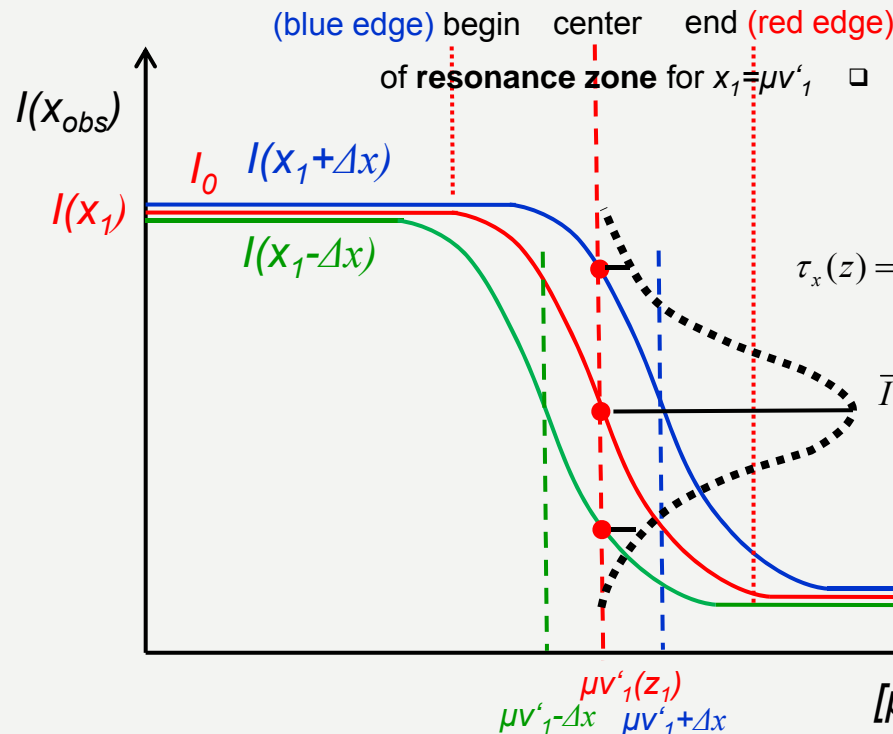
$$\bar{I}(z_1) = \int I_\nu(x,z_1) \, \phi(x-\mu v'_1,z_1) \, dx \qquad x \text{ varies}$$

$I_0 \exp[-\tau_x(z_{end})]$ for pure abs.

$[\mu v'](z)= \mu(z)v'(r(z))$, i.e.,$v'>0$ always (for outflows)

From the slides before, it is evident that line processes (contrasted to continuum ones) occur in a very localized region in the wind. V. Sobolev (1960; but work done during world-war II) was the first to obtain a completely local approximation which is quite close to reality (and can be extended to become even more precise).
The following derivation follows (in part) Owocki & Puls (1996);
for an alternative derivation (very insightful), see Rybicki & Hummer (1978)

For simplicity, in the following

(i) we concentrate on outflows, i.e., $v(r) > 0$ [though $dv/dr < 0$ is not excluded],

(ii) adopt, as before, a spatially constant thermal speed $v_{th}(r) = v_{th}$, and

(iii) define $\chi_1(r) = \dfrac{\overline{\chi}_L(r)}{\Delta v_D}$

The optical depth difference (along impact parameter $p$) between two points $z_1$ and $z_2$ is given by

$$t(x, p, z_1, z_2,) = \int_{\min(z_1,z_2)}^{\max(z_1,z_2)} \chi_1(r')\phi\big(x - \mu' v'(r')\big)\,dz' \quad \text{with (as usual)} \ \mu' = \frac{z'}{r'}, \ \text{and} \ r' = \sqrt{z'^2 + p^2}. \ \text{Then, without any approx.,}$$

$$I_v(x, p, z) = \underbrace{I_{core}e^{-t(x,p,z,z_B)}}_{\substack{\text{direct component, only present} \\ \text{for } \mu>0 \text{ and } p\leq R_*}} + \underbrace{\int_0^{t(x,p,z,z_B)} S(r')e^{-t(x,p,z,z')}\,dt(x,p,z,z')}_{\text{diffuse component (from radiation scattered or emitted in the wind)}} \quad \text{with } z_B = \begin{cases} z_* \ \text{for } z > 0, \ p \leq R_* \\ -\infty \ \text{else} \end{cases}$$

The above equation is valid for both outward ($\mu \geq 0$) and inward ($\mu < 0$) directed rays, in dependence of the sign of $z$.

Here, we use a p-z geometry extending over both hemispheres, with $z > 0$ for the front and $z < 0$ for the back hemisphere!

$$I_\nu(x,p,z) = \underbrace{I_{core}e^{-t(x,p,z,z_B)}}_{\substack{\text{direct component, only present}\\\text{for } \mu>0 \text{ and } p \leq R_*}} + \underbrace{\int_0^{t(x,p,z,z_B)} S(r')e^{-t(x,p,z,z')}dt(x,p,z,z')}_{\text{diffuse component (from radiation scattered or emitted in the wind)}} \quad \text{with } z_B = \begin{cases} z_* & \text{for } z>0, \ p \leq R_* \\ -\infty & \text{else} \end{cases}$$

To calculate the scattering integrals, we first integrate over $\phi(x)dx$

$$\bar{I}(\mu,r) = \int_{-\infty}^{+\infty} I_\nu(x,\mu,r)\phi\big(x-\mu v'(r)\big)dx \quad \text{and then over } d\mu,$$

**This is the Sobolev approximation: opacities (and source functions) are assumed to be constant over the resonance zone**

$$\bar{J}(r) = \frac{1}{2}\int_{-1}^{+1} \bar{I}(\mu,r)d\mu$$

Now we consider that the integrands provide a contribution only if $x \approx \mu'v'(r')$ or $x \approx \mu v'(r)$, respectively, due to the behaviour of $\phi$. For the optical depth difference,

$$t(x,p,z,z_B,) = \int_{\min(z,z_B)}^{\max(z,z_B)} \chi_l(r')\phi\big(x-\mu'v'(r')\big)dz' \quad \to \chi_l(r_0)\int_{z_{min}}^{z_{max}} \phi\big(x-\mu'v'(r')\big)dz',$$

where $r_0$ is the position of the corresponding resonance zone, and needs to be calculated from

$$[\mu v'](r_0) = x, \ \text{ i.e., } \pm\sqrt{1-\frac{p^2}{r_0^2}}v'(r_0) = x \ \text{ (non-linear eq.)},$$

which has a unique solution for strictly monotonic flows (otherwise there is more than one resonance zone).

Moreover, we switch from an integration over $\mathrm{d}z'$ to an integration over CMF-frequency,

$$\mathrm{d}x_{\mathrm{CMF}} = \mathrm{d}(x - \mu v'(r'))$$

$$\left.\frac{\mathrm{d}x_{\mathrm{CMF}}}{\mathrm{d}z}\right|_p = -\left.\frac{\mathrm{d}(\mu v')}{\mathrm{d}z}\right|_p = (\text{see } \underline{\text{slide 23}}) = -\left(\mu^2 \frac{\mathrm{d}v'}{\mathrm{d}r} + (1-\mu^2)\frac{v'}{r}\right) =: -Q(r,\mu). \quad \text{For } Q > 0,$$

by considering boundaries: $x_{\mathrm{CMF}}(z) = x - \mu v'(r)$, $x_{\mathrm{CMF}}(z_B) \to \infty$ [blueward of blue edge of resonance zone], and by putting $Q(r,\mu)$ in front of the integral [same argument as before], we arrive at

$$t(x,p,z,z_B) \approx \chi_l(r_0) \int_{x_{\mathrm{CMF}}(z_B)}^{x_{\mathrm{CMF}}(z)} \frac{-1}{Q(r',\mu')}\phi(x_{\mathrm{CMF}})\mathrm{d}x_{\mathrm{CMF}} \to \frac{\chi_l(r_0)}{Q(r_0,\mu_0)}\int_{x-\mu v'(z)}^{\infty}\phi(\xi)\mathrm{d}\xi = \tau_S(r_0,\mu_0)\Phi(x-\mu v'(r))$$

This result can be generalized for positive and negative values of Q, if we define

$$\boxed{\tau_S(r_0,\mu_0) = \frac{\chi_l(r_0)}{|Q(r_0,\mu_0)|} = \frac{\bar\chi_L(r_0)}{\Delta\nu_D\left|\mu^2\dfrac{\mathrm{d}v'}{\mathrm{d}r} + (1-\mu^2)\dfrac{v'}{r}\right|_{r_0,\mu_0}}}$$

In the general case, $Q$ is the directional derivative of the velocity in direction $\mathbf{n}$, i.e., $|Q| = |\mathbf{n}\cdot\nabla(\mathbf{n}\cdot\mathbf{v}')| = \left|\dfrac{\mathrm{d}v'_l}{\mathrm{d}l}\right|$ if $l$ has direction $\mathbf{n}$

as the Sobolev optical depth, evaluated at the resonance zone.

NOTE1: $\Phi(\infty)=0$ [blue(starward) side of resonance zone], $\Phi(-\infty)=1$ [red side of resonance zone]

(remember: v > 0)

thus: $t(x,p,z,z_B) \to 0$ for $z$ "before" resonance zone, $I(t)=I_{core}$  $\Big\}$ see slides 23 / 24

$\quad\quad t(x,p,z,z_B) \to \tau_S$ for $z$ "behind" resonance zone, $I(t) \approx I_{core}\exp(-\tau_S)$

NOTE2: for pure Doppler-profiles, $\Phi(x)=\dfrac{1}{2}\operatorname{erfc}(x)$

NOTE3: since v' is the velocity in units of the thermal speed, and since $\Delta\nu_D = \dfrac{v_{th}}{\tilde{\lambda}}$, we can

alternatively write

$$\tau_S(r_0,\mu_0) \;=\; \frac{\bar{\chi}_L(r_0)\tilde{\lambda}}{\left|\mu^2\dfrac{dv}{dr}+(1-\mu^2)\dfrac{v}{r}\right|_{r_0,\mu_0}}$$  when v and $r$ are measured in actual units (then, $[v/r]=s^{-1}$)

Since also the integrand of the diffuse component contributes only for $x \approx \mu'v'$,

$$\int_0^{t(x,p,z,z_B)} S(r')e^{-t(x,p,z,z')}dt(x,p,z,z') \rightarrow S(r_0)\int_0^t e^{-t'}dt' = S(r_0)\left(1-e^{-t(x,p,z,z_B)}\right),$$

the specific intensity can be approximated by

$$I_\nu(x,p,z) \approx I_{\text{core}}(p)\, e^{-\tau_S(r_0,\mu_0)\Phi(x_{\text{CMF}})} + S(r_0)\left(1-e^{-\tau_S(r_0,\mu_0)\Phi(x_{\text{CMF}})}\right)$$

This means that behind the resonance zone (where $\Phi(x_{\text{CMF}})=1$)

$$I_\nu(x,p,z_{\text{behind}}) \approx I_{\text{core}}(p)\, e^{-\tau_S(r_0,\mu_0)} + S(r_0)\left(1-e^{-\tau_S(r_0,\mu_0)}\right) = \text{const}$$

whilst before the resonance zone (where $\Phi(x_{\text{CMF}})=0$)

$$I_\nu(x,p,z_{\text{before}}) \approx \begin{cases} I_{\text{core}}(p) = \text{const for } p \leq R_* \\ 0 \quad \text{else} \end{cases}$$

compare with <u>slides 23</u> / <u>24</u>

Only inside the resonance zone, the optical depth increases, and the intensity varies accordingly!

To calculate the intensity in Sobolev approximation (required, e.g., for the emergent profile), the location of the resonance zone has to be evaluated for each frequency and impact parameter!

Now comes the 2nd "trick" .... As outlined, we first calculate

$$\bar{I}(r,\mu) = \int_{-\infty}^{+\infty} \left[ I_{\text{core}}(p) \, e^{-\tau_S(r_0,\mu_0)\Phi(x_{\text{CMF}})} + S(r_0) \left( 1 - e^{-\tau_S(r_0,\mu_0)\Phi(x_{\text{CMF}})} \right) \right] \phi(x_{\text{CMF}}(r,\mu)) \, dx$$

Again, we find a contribution only for $x_{\text{CMF}} \approx 0$, i.e., $x \approx \mu v'(r)$.

Thus, we can replace $r_0$ by $r$ and $\mu_0$ by $\mu$; realizing that

$$\phi(x_{\text{CMF}}) \, dx = -d\Phi$$

with $\Phi(x_{\text{CMF}} = x - \mu v') \rightarrow 1$ for $x \rightarrow -\infty$

and $\Phi(x_{\text{CMF}} = x - \mu v') \rightarrow 0$ for $x \rightarrow +\infty$, we find

$$\bar{I}(r,\mu) \approx \int_0^1 \left[ I_{\text{core}}(p) \, e^{-\tau_S(r,\mu)\Phi(x_{\text{CMF}})} + S(r) \left( 1 - e^{-\tau_S(r,\mu)\Phi(x_{\text{CMF}})} \right) \right] d\Phi =$$

$$= I_{\text{core}}(p) \frac{1 - e^{-\tau_S(r,\mu)}}{\tau_S(r,\mu)} + S(r) \left( 1 - \frac{1 - e^{-\tau_S(r,\mu)}}{\tau_S(r,\mu)} \right),$$

which is already PURELY LOCAL.

$$\bar{I}(r,\mu) = I_{\text{core}}(p)\frac{1-e^{-\tau_S(r,\mu)}}{\tau_S(r,\mu)} + S(r)\left(1 - \frac{1-e^{-\tau_S(r,\mu)}}{\tau_S(r,\mu)}\right)$$

Finally, by integrating over $d\mu$, and accounting for the limits regarding the first term,

$$\bar{J}(r) = \beta_c(r)I_{\text{core}} + \left(1-\beta(r)\right)S(r)$$

with

$$\beta_c(r)I_{\text{core}} = \frac{1}{2}\int_{\mu_*}^{1} I_{\text{core}}(\mu,\bar{\nu})\frac{1-e^{-\tau_S(r,\mu)}}{\tau_S(r,\mu)}\,d\mu \quad \text{and escape probability} \quad \beta(r) = \frac{1}{2}\int_{-1}^{1}\frac{1-e^{-\tau_S(r,\mu)}}{\tau_S(r,\mu)}\,d\mu.$$

Note that

(i) the core intensity has to be emitted (evaluated) at the core with an observer's (rest) frame frequency of $\bar{\nu} \approx \tilde{\nu}\left(1+\mu v(r)/c\right)$ (corresponding to $x_{\text{CMF}}=0$, i.e., $x=\mu v'$), in order to display a CMF-frequency of $\nu_{\text{CMF}} \approx \tilde{\nu}$ at $(\mu, v(r))$.

This ensures that the resonance zone is illuminated by the full core-intensity (deshadowing!)

(ii) the angular integration does NOT require a highly resolved angular grid

(since the interaction between $x, \mu$, and $r$ has been already accounted for)

1. Sobolev optical depth for resonance lines

Had $\tau_S(r_0,\mu_0) = \dfrac{\chi_o(r_0)}{|Q(r_0,\mu_0)|} = \dfrac{\overline{\chi}_L(r_0)}{\Delta\nu_D\left|\mu^2\dfrac{dv'}{dr}+(1-\mu^2)\dfrac{v'}{r}\right|_{r_0,\mu_0}}$ → for radial rays ($\mu=1$) $\tau_S(r) \propto \dfrac{\overline{\chi}_L(r)}{\dfrac{dv}{dr}}$

(UV) resonance lines: $\overline{\chi}_L(r) \propto n_1(r) \propto \rho(r)$ if ground-state of main ionization stage;

with $\rho(r) = \dfrac{\dot{M}}{4\pi r^2 v(r)}$ , we obtain

$\tau_S(r) \propto \dfrac{1}{r^2 v(r)\dfrac{dv}{dr}} = \dfrac{1}{\beta b R_* v_\infty^2}\left(\dfrac{v(r)}{v_\infty}\right)^{\frac{1}{\beta}-2}$ $\Rightarrow$ $\tau_S(r) = const$ for $\beta=0.5$, and $\boxed{\tau_S(r) \propto \dfrac{v_\infty}{v(r)} \text{ for } \beta=1}$ ,

i.e., a decrease by roughly (and only) a factor of 100 from inside to outside.

This means that a strong UV-line (e.g., CIV 1548/1550, Fig. 1) will remain optically thick thoughout the complete wind!!!!

2. Source function for a pure scattering resonance line

In Chap. 4, we will show that in this case $S(r) = \bar{J}(r) = \dfrac{\beta_c(r) I_{core}}{\beta(r)}$

a) optically thin limit, $\tau_S(r) \ll 1$ $\Rightarrow \dfrac{1 - e^{-\tau_S(r)}}{\tau_S(r)} \to 1$ and $S(r) = \dfrac{\beta_c(r) I_{core}}{\beta(r)} \to W I_{core}$ with dilution factor $W$

$\Rightarrow \left(\dfrac{r}{R_*}\right)^2 S(r) \to \dfrac{I_{core}}{4} = const$ for large radii, i.e., $\boxed{S(r) \propto \left(\dfrac{R_*}{r}\right)^2}$ quadratic dilution!

[compare with slide 14 : consistent, since optically thin line $\Rightarrow \bar{J} = J$, and $J = W I_{core} \Rightarrow S = W I_{core}$ ]

b) optically thick limit, $\tau_S(r) \gg 1$ $\Rightarrow \dfrac{1 - e^{-\tau_S(r)}}{\tau_S(r)} \to \dfrac{1}{\tau_S(r)}$

and $S(r) = \dfrac{\beta_c(r) I_{core}}{\beta(r)} \to \left(\dfrac{R_*}{r}\right)^2 I_{core} \dfrac{3}{4 + 8\left(\dfrac{d \ln v}{d \ln r}\right)^{-1}}$ for large radii

$\Rightarrow \boxed{S(r) \propto \left(\dfrac{R_*}{r}\right)^3}$ for large radii, i.e.,

the source function goes faster to zero than in the optically thin case

The approximate radiative line acceleration due to ONE line is provided by

$$g_{rad} = \frac{4\pi}{c} \frac{\overline{\chi}_L}{\rho} \frac{1}{2} \int \overline{I}(\mu)\mu d\mu \approx \frac{2\pi}{c} \frac{\overline{\chi}_L}{\rho} \int_{\mu_*}^1 I_{core}(\mu,\overline{v}) \frac{1-e^{-\tau_S(r,\mu)}}{\tau_S(r,\mu)} \mu d\mu,$$

since the contribution from the source term (even in $\mu$) cancels when integrating over $\mu d\mu$ with $\mu \in [-1,1]$.

Note that $g_{rad} \propto \dfrac{\overline{\chi}_L}{\rho}$ and not $\dfrac{\overline{\chi}_L}{\rho \Delta v_D}$ [see Appendix B]

In the optically thick case ($\tau_S = \dfrac{\overline{\chi}_L}{\Delta v_D |Q(r,\mu)|} \gg 1$), $g_{rad} \xrightarrow{\tau_S \gg 1} \dfrac{2\pi}{c} \dfrac{\overline{\chi}_L}{\rho} \dfrac{1}{\overline{\chi}_L/\Delta v_D} \int_{\mu_*}^1 I_{core}(\mu,\overline{v})|Q(r,\mu)| \mu d\mu,$

and the line acceleration becomes independent of $\overline{\chi}_L$,

$$\boxed{g_{rad} \xrightarrow{\tau_S \gg 1} \frac{2\pi}{c\rho} \Delta v_D \int_{\mu_*}^1 I_{core}(\mu,\overline{v})|Q(r,\mu)| \mu d\mu}, \quad \text{with } |Q(r,\mu)| = \left| \mu^2 \frac{dv'}{dr} + (1-\mu^2)\frac{v'}{r} \right|$$

The *Sobolev length* is roughly the (half-)width of the resonance zone.
More precisely, it is the length scale where *v(r)* changes by 1 $v_{th}$, accounting for the most decisive part of the profile function:

$$\Delta v = v_{th} := \left| \frac{dv}{dr} \right| L_{Sob} \qquad \Rightarrow \qquad \boxed{L_{Sob} = \frac{v_{th}}{|dv/dr|}} = \frac{1}{|dv'/dr|} \quad \text{for radial rays}$$

$$\Delta v = v_{th} := \left| \frac{d(\mu v)}{dz} \right| L_{Sob} \qquad \Rightarrow \qquad L_{Sob} = \frac{v_{th}}{\left| \mu^2 \frac{dv}{dr} + (1-\mu^2)\frac{v}{r} \right|} = \frac{1}{\left| \mu^2 \frac{dv'}{dr} + (1-\mu^2)\frac{v'}{r} \right|} \quad \text{for spherical symmetry}$$

most generally: $L_{Sob} = \frac{v_{th}}{|\mathbf{n} \cdot \nabla(\mathbf{n} \cdot \mathbf{v})|}$ in direction $\mathbf{n}$

For small $v_{micro}$, $L_{Sob}$ depends on $m_{ion}^{-1/2}$

Let's define a characteristic length scale, $l_x$, for a macro-variable $x$, defined via

$$\frac{dx}{dr} l_x = x, \text{ i.e., } l_x = \left(\frac{d \ln x}{dr}\right)^{-1}$$

To warrant the validity of the Sobolev approximation (SA), $L_{\text{Sob}}$ must be smaller than $l_x$,

$$\left|\frac{L_{\text{Sob}}}{l_x}\right| = \left|\frac{d \ln x}{dv/v_{\text{th}}}\right| < 1$$

Example: let's consider the opacity (previously assumed as being roughly constant over the resonance zone when evaluating the optical-depth integrals).

For (UV-) resonance lines, $\bar{\chi}_L(r) \propto \rho(r)$, and a typical velocity field reads $v(r) = v_\infty (1 - \frac{R_*}{r})^\beta$

with $\beta = 1$. Then,

$$\left|\frac{L_{\text{Sob}}}{l_{\bar{\chi}}}\right| = \frac{v_{\text{th}}}{v} + \frac{2v_{\text{th}}}{v_\infty}\frac{r}{R_*}$$

Thus, the Sobolev approximation is valid (regarding an opacity propto ρ)
i.    as long as $v(r) > v_{\text{th}}$, and
ii.   as long as $r/R_* < v_\infty/(2v_{\text{th}}) = O(100)$, i.e., for all relevant radii

As it turns out, a similar condition applies for the source-function.
The only regions where the SA fails is

❑ the sub-thermal region (density decreases exponentially within a very extended resonance zone), and

❑ the transition zone between quasi-hydrostatic photosphere and wind, where the resonance zone is still broad, however the velocity-field has a significant curvature (and not a constant gradient).
[Unfortunately, this zone is very important regarding the radiative line-acceleration, and is badly described when using the SA (see Owocki & Puls 1999)]

❑ Interestingly, the SA is almost perfectly valid in a Supernova remnant, due to a velocity field v ~ r, i.e., a constant gradient

Note also that the SA fails in a correct description of the reaction of the line acceleration onto disturbances. Most important, the so-called line-driven instability (LDI) cannot be represented in the framework of SA.

❏ Coupling with continuum: Hummer & Rybicki 1985

❏ Important when continuum is no longer optically thin

$$\bar{J}(r) = \overline{\beta_c(r)I_{inc}} + \left(1-\beta(r)\right)S_L(r) + \left(S_c(r)-S_L(r)\right)\bar{U}(\tau_S,\beta_P)$$

with $\overline{\beta_c(r)I_{inc}} = \dfrac{1}{2}\displaystyle\int_{-1}^{1} I^{inc}(r,\mu)\dfrac{1-e^{-\tau_S(r,\mu)}}{\tau_S(r,\mu)}d\mu,$ and $I^{inc}(r,\mu)$ the intensity incident at the considered

location (resonance zone), usually the continuum intensity;

$\beta(r)$ is the $\left(\text{conventional}\right)$ escape probability, $S_c(r)$ the continuum source-function, and $\bar{U}(\tau_S,\beta_P)$ is a function

describing the actual coupling of the opacities in the resonance zone, with $\beta_P = \dfrac{\chi_c}{\bar{\chi}_L/\Delta\nu_D}$ the ratio of continuum

and line opacity. The function $\bar{U}$ can be obtained, e.g., from pre-calculated tables (Taresch et al. 1997).

Often, the last term can be neglected, but at least the first term (modified compared to the previous expression)
needs to be considered when the continuum is non-neglibile ...

... either one uses the intensities from the continuum transfer, or applies the following reasoning (unpublished thus far):

$$\overline{\beta_c(r)I_{inc}} = \frac{1}{2}\int_{-1}^{1} I^{inc}(r,\mu)\frac{1-e^{-\tau_S(r,\mu)}}{\tau_S(r,\mu)}d\mu \quad\xrightarrow{\tau_S \gg 1,\ dv/dr>0}\quad \frac{1}{2\chi_0}\int_{-1}^{1} I^{inc}(r,\mu)\left[\mu^2\frac{dv'}{dr} + (1-\mu^2)\frac{v'}{r}\right]d\mu =$$

$$= \frac{1}{\chi_0}\left[K_\nu(r)\left(\frac{dv'}{dr}-\frac{v'}{r}\right) + J_\nu(r)\frac{v'}{r}\right] = \frac{1}{\chi_0}J_\nu(r)\left[f_\nu(r)\left(\frac{dv'}{dr}-\frac{v'}{r}\right)+\frac{v'}{r}\right]$$

$$= J_\nu(r)\frac{1}{\tau_S(r,\mu=\sqrt{f_\nu(r)})},\ \text{where } f_\nu(r)=\frac{K_\nu}{J_\nu}\ \text{ is the Eddington factor.}$$

Accounting also for the optically thin case, one finds to a good approximation

$$\boxed{\overline{\beta_c(r)I_{inc}} \approx J_\nu(r)\frac{1-e^{-\tau_S(r,\mu=\sqrt{f_\nu(r)})}}{\tau_S(r,\mu=\sqrt{f_\nu(r)})}}\quad,\text{ and avoids the angular integration}$$

by evaluating the SA-optical depth at $\mu=\sqrt{f_\nu(r)}$.

A similar reasoning yields an approximation for the escape probability,

$$\boxed{\beta(r) \approx \frac{1-e^{-\tau_S(r,\mu=\sqrt{1/3})}}{\tau_S(r,\mu=\sqrt{1/3})}}$$

❑ **Inclusion of source-function gradients:** Sobolev 1957, Castor 1974, Puls & Hummer 1988

  ❑ important when calculating the line-acceleration:
  constant source function does not contribute, but gradient does (see also Owocki & Puls 1999); inclusion of continuum terms essential.

❑ **Inclusion of multi-line effects:** Puls 1987 (see also Friend & Castor 1983)

  ❑ important when calculating the **total** line-acceleration, $\Sigma_i \, g^i_{rad}$
  ❑ different lines can interact with each other, due to Doppler-induced frequency shifts

  e.g., for the same $v_{obs}$, there might be an interaction with a line at $\tilde{\nu}_1$ in the inner wind,

  and subsequently in the more outer part with a line at $\tilde{\nu}_2 < \tilde{\nu}_1$, if $\dfrac{\tilde{\nu}_1 - \tilde{\nu}_2}{\tilde{\nu}_1} \approx \dfrac{(\mu v)_2}{c} - \dfrac{(\mu v)_1}{c}$

  In other words, the radiation incident at $(\mu v)_2$ (determining the radiation field for $\tilde{\nu}_2$)

  has already been processed before, by line $\tilde{\nu}_1$ at $(\mu v)_1$

❑ **Incl. of non-monotonic velocity fields:** Puls, Owocki & Fullerton 1996

  ❑ more than one resonance zone,
  important when calculating line-acceleration in time-dependent winds
  prone to the LDI (line-driven instability)

When calculating line-profiles (specifically, UV P Cygni lines) and using the SA exclusively (i.e., to determine the source function AND the emergent profile), the accuracy – compared to "exact" methods – is quite low.

A better approach is to calculate the scattering integral (and thus the source-function, either in a complete NLTE or a two-level-approach) using the SA, and then to derive the emergent line profile from an "exact" formal solution using such source-function.

First noted by Hamann (1981), and explicitly suggested by Lamers et al. (1987): "SEI" [independently used by Puls 1987, for the case of a large number of overlapping lines, in the context of NLTE wind modeling/spectrum synthesis]
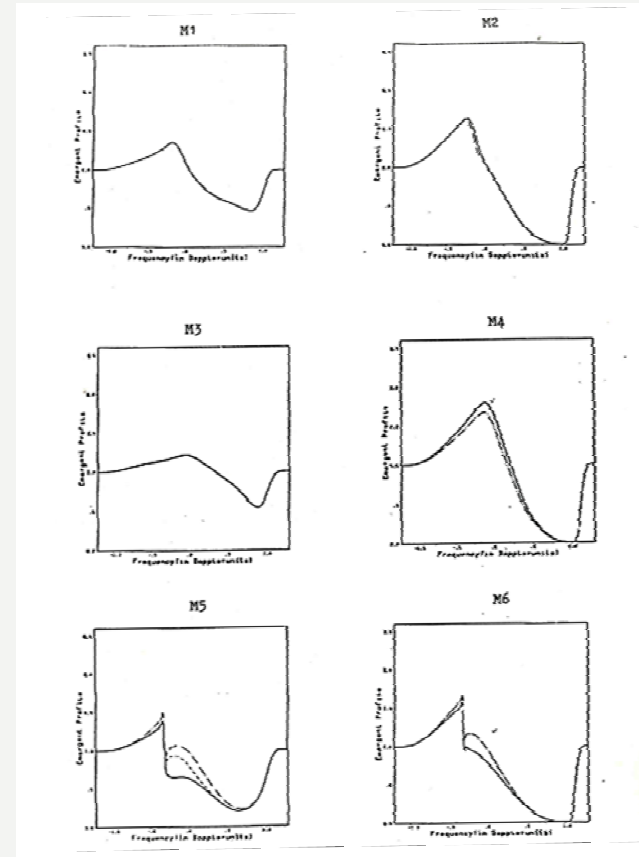


emergent profiles with $S=\bar{J}$, for intermediate (left) and strong (right) wind lines, and different opacity stratifications. Solid: 'exact' (CMF), dashed-dotted: SEI. From Puls (1985, Diploma Thesis).
Note: Blue frequencies on the right!
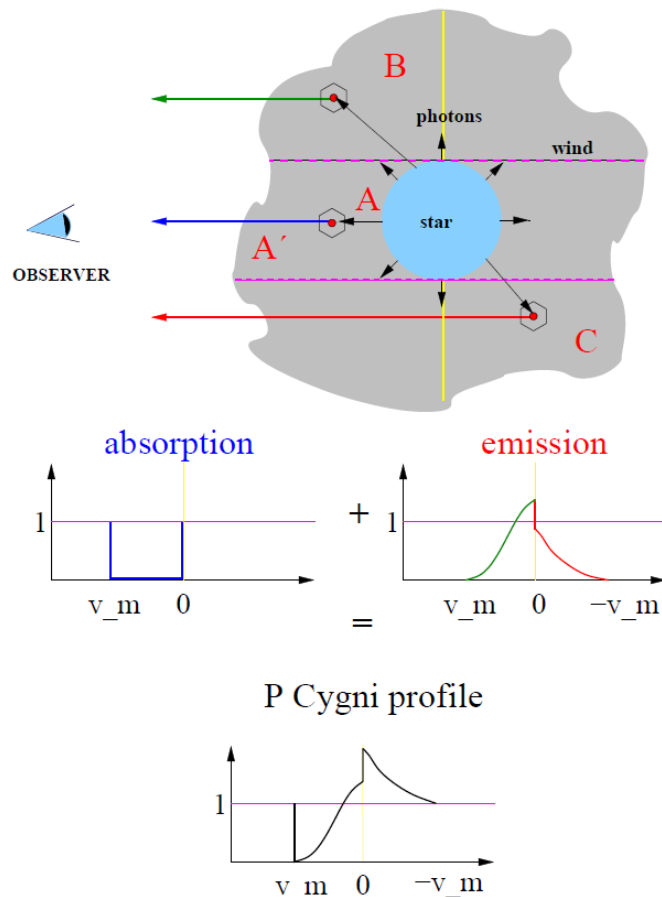
… assuming a strong resonance line, remaining optically thick until v_m (corresponding to the terminal velocity)

due to Dopplershifts, all obs. frame frequencies corresponding to [+v_m, -v_m] can contribute

absorption in region A in front of stellar disk (approaching material → blue frequencies )

asymmetric emission from region A'/B in front hemisphere (blue emission due to approaching material), and region C (side lobes) in back hemisphere (red emission due to receding material).

emission caused by line scattering

When calculating the formal solution via an integral method, it is advantageous to remap all quantities onto a micro-grid of resolution ≈ $v_{th}/3$, to ensure a correct treatment of the resonance zone (e.g., Santolaya-Rey et al. 1997)

Obviously, the calculation of the radiation field in an environment
with significant (supersonic) velocity-fields is either

- time-consuming, if done in the observer's frame:
  many grid-points, frequencies, and angles, or
- only approximate (but fast), when done using the Sobolev-approximation:
  additional difficulties when considering not only one isolated line in an
  optically thin continuum, but more realistic cases as occurring in NLTE-
  atmosphere calculations (many lines, various continua, multi-line effects …)

A simple solution is possible when the velocity field is monotonic,
after transforming to the comoving frame

Note: a CMF-solution is also possible for non-monotonic velocity fields, at least
      in principle, but the algorithm becomes very complex.

We start in the observer's frame, using the p-z geometry (now again for the front hemisphere only)

$$\pm \frac{dI^{\pm}(z,p,\nu)}{dz} = \eta_{\nu}\left(r, \nu(1-\frac{\mu v}{c})\right) - \chi_{\nu}\left(r, \nu(1-\frac{\mu v}{c})\right) I^{\pm}(z,p,\nu),$$

where in the following all CMF quantities are denoted by a sub-(or super-)script '0'; e.g., $\nu_0 \triangleq \nu_{CMF} = \nu(1-\frac{\mu v}{c})$

A velocity field produces Doppler-shifts, aberration and advection terms (see below); formally, all of these are $O(v/c)$, but for lines the Doppler shifts become signficant already if $v = O(v_{th})$, due to the rapid change of the profile function. Thus, in a heuristic approach, let's concentrate on the Doppler-shifts, and neglect the rest [see also Lucy 1971]

Since $\nu_0 = \nu_0(\nu,z) = \nu(1-\frac{\mu v}{c})$, the spatial derivative needs to account for the change of $\nu_0$ with $z$:

$$\left.\frac{d}{dz}\right|_{\nu} = \left.\frac{\partial}{\partial z}\right|_{\nu_0} + \left.\frac{\partial}{\partial \nu_0}\right|_{z_0} \left.\frac{\partial \nu_0}{\partial z}\right|_{\nu} \quad \text{with} \quad \left.\frac{\partial \nu_0}{\partial z}\right|_{\nu} = -\frac{\nu}{c}\frac{\partial(\mu v)}{\partial z} \stackrel{O(v/c)}{\approx} \mp \frac{\nu_0}{c}\tilde{Q}(r,\mu)$$

[we approximate $r \approx r_0$ and $\mu \approx \mu_0$, and account for the fact that when using $z > 0$ exclusively, $\frac{\partial(\mu v)}{\partial z} = \pm \tilde{Q}(r,\mu)$ for $\mu > 0$ and $\mu < 0$, respectively;

$\tilde{Q}$ evaluated using v instead of v']

$$\left.\frac{d}{dz}\right|_{\nu=const} = \left.\frac{\partial}{\partial z}\right|_{\nu_0=const} + \left.\frac{\partial \nu_0}{\partial z}\right|_{\nu} \left.\frac{\partial}{\partial \nu_0}\right|_{z_0=const}$$



$$\nu_{CMF} = \nu_{obs}\left(1-\frac{\mu v}{c}\right)$$

$$\nu_{obs} \approx \nu_{CMF}\left(1+\frac{\mu v}{c}\right)$$

$\nu_{obs} = const$

$\nu_{CMF} = const$

sketch for μ>0
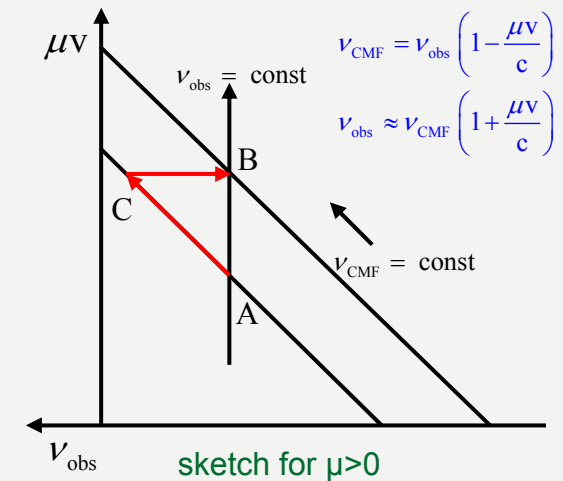
observer's frame: $(A) \stackrel{v=const}{\rightarrow} (B) \triangleq$ CMF: $(A) \stackrel{\nu_0=const}{\rightarrow} (C) + (C) \stackrel{z_0 \approx z=const}{\rightarrow} (B)$

Thus, the RTE becomes

... in p-z geometry with $r_0 \approx r$, $\mu_0 \approx \mu$, $z_0 \approx z$

$$\pm \frac{\partial I_0^{\pm}(z, p, \nu_0)}{\partial z} - \frac{\nu_0 \tilde{Q}(r, \mu)}{c} \frac{\partial I_0^{\pm}(z, p, \nu_0)}{\partial \nu_0} = \eta_0(r, \nu_0) - \chi_0(r, \nu_0) I_0^{\pm}(z, p, \nu_0)$$

NOTE: Whilst the first (spatial) derivative enters with $'\pm'$ for outward and inward radiation, respectively, the 2nd (frequency) derivative has the same sign in both cases. This again is due to the fact that the gradient of $\mu\nu$ is always positive in a spherically expanding medium (as long as $\nu(r)$ is monotonically increasing), irrespective of direction.

... in spherical geometry/symmetry with $r_0 \approx r$, $\mu_0 \approx \mu$

$$\mu_0 \frac{\partial I_0(r, \mu_0, \nu_0)}{\partial r} + \frac{1 - \mu_0^2}{r} \frac{\partial I_0(r, \mu_0, \nu_0)}{\partial \mu_0} - \frac{\nu_0 \tilde{Q}(r, \mu_0)}{c} \frac{\partial I_0(r, \mu_0, \nu_0)}{\partial \nu_0} = \eta_0(r, \nu_0) - \chi_0(r, \nu_0) I_0(r, \mu_0, \nu_0)$$

... and in plane-parallel symmetry with $z_0 \approx z$, $\mu_0 \approx \mu$

$$\mu_0 \frac{\partial I_0(z, \mu_0, \nu_0)}{\partial z} - \frac{\nu_0 \mu_0^2 (d\nu/dz)}{c} \frac{\partial I_0(z, \mu_0, \nu_0)}{\partial \nu_0} = \eta_0(z, \nu_0) - \chi_0(z, \nu_0) I_0(z, \mu_0, \nu_0)$$

- The full transformation of the RTE for non-uniform velocity fields (including time-dependent terms) can be found, e.g., in Castor (1972)
- Mihalas, Kunasz & Hummer (1976) showed that aberration terms (involving changes in direction μ) and advection terms (arising 'from gradients or from a "sweeping up" of radiation by the transformation' to the CMF) can be neglected when v<<c (as considered here; but SN-remnants!), whilst the frequency derivatives are most important. Thus far, the above equations are sufficient as long as v<<c.

- in the above equations, particularly $I_0$, $\eta_0$, and $\chi_0$ are in the comoving frame, and $\eta_0$ and $\chi_0$ are isotropic
- consequently, for each line (if treated as a single one), only a small frequency range covering the variation of $\Phi$ ($\approx \pm 3$ $v_{th}$) needs to be considered.
- if only *one* line considered, RT performed exclusively in the resonance zone

- The CMF RTE is a partial differential equation (PDE) of hyperbolic type, and poses an initial boundary value problem, i.e., requires boundary conditions in space and initial values in frequency
- for larger frequency ranges, it might be useful to differentiate via

$$\frac{v_0 \tilde{Q}(r,\mu)}{c} \frac{\partial}{\partial v_0} = \frac{\tilde{Q}(r,\mu)}{c} \frac{\partial}{\partial \ln v_0}$$

$$\pm\frac{\partial I_0^{\pm}(z,p,\nu_0)}{\partial z} - \frac{\nu_0 \tilde{Q}(r,\mu)}{c}\frac{\partial I_0^{\pm}(z,p,\nu_0)}{\partial \nu_0} = \eta_0(r,\nu_0) - \chi_0(r,\nu_0)I_0^{\pm}(z,p,\nu_0)$$

Let's use Doppler-units w.r.t. $v_\infty$, $x_0 = \dfrac{\nu_0 - \tilde{\nu}}{\Delta\nu_\infty}$ and $\Delta\nu_\infty = \dfrac{\nu_0 v_\infty}{c}$, where $\tilde{\nu}$ is an arbitrary reference frequency close to $\nu_0$.

Measuring v in units of $v_\infty$ ($v'' = v/v_\infty$), and accounting for $dx_0 = \dfrac{c}{v_\infty}\dfrac{\tilde{\nu}}{\nu_0}\dfrac{d\nu_0}{\nu_0} \approx \dfrac{c}{v_\infty \nu_0}d\nu_0 = \dfrac{d\nu_0}{\Delta\nu_\infty}$, we find

$$\pm\frac{\partial I_0^{\pm}(z,p,x_0)}{\partial z} - P(r,\mu)\frac{\partial I_0^{\pm}(z,p,x_0)}{\partial x_0} = \eta_0(r,x_0) - \chi_0(r,x_0)I_0^{\pm}(z,p,x_0) \quad \text{with } P(r,\mu) = \frac{d(\mu v'')}{dz} = \left(\mu^2\frac{dv''}{dr} + (1-\mu^2)\frac{v''}{r}\right)$$

The characteristics of the homogeneous (r.h.s. $= 0$) PDE are the curves (generally:

hypersurfaces) along which $I_0^{\pm}$ remains constant if there is no absorption/emission.
For the type of PDE considered here, they are given by (consult literature)

$$\frac{dx_0}{dz} = \mp P(z), \quad \text{and integration results in}$$

$$0 < \Delta x_0 = x_{0,B} - x_0 = \mp\int_z^{z_B} P(z)\,dz = \mp\left[\mu v''(z_B) - \mu v''(z)\right] = \mp\Delta\mu v''. \quad \text{Thus,}$$

$$\boxed{I_0^{\pm}(\mu v''(z),x_0) = I_0^{\pm}(\mu v''(z_B),x_{0,B}) = I_0^{\pm}(\mu v''(z)\mp\Delta x_0, x_0 + \Delta x_0).}$$

Without absorption and emission, **all** photons are 'only' redshifted w.r.t. the CMF,
from $x_0 + \Delta x_0$ to $x_0$, both when propagating outward from $\mu v''(z) - \Delta x_0$ to $\mu v''(z)$,
and when propagating inward from $\mu v''(z) + \Delta x_0$ to $\mu v''(z)$.

[The corresponding observer's frame intensity at $x$, $I^{\pm}(z,x)$, remains constant, of course].



$\dfrac{dx_0}{dz} = \mp P$, i.e.,

$\Delta x_0 = \mp P\Delta z = \mp\Delta\mu v''$

$\Rightarrow$ slope $\dfrac{d\mu v''}{dx_0} = \mp 1$
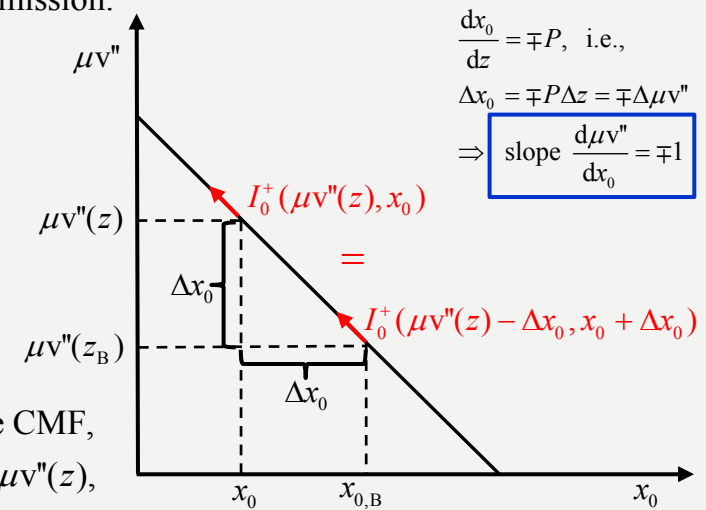
sketch for μ>0

From the CMF-RTE,

$$\pm\frac{\partial I_0^{\pm}(z,p,x_0)}{\partial z} - P(r,\mu)\frac{\partial I_0^{\pm}(z,p,x_0)}{\partial x_0} = \eta_0(r,x_0) - \chi_0(r,x_0)I_0^{\pm}(z,p,x_0),$$

one can also derive the Sobolev limit without problems.

Since we are in the CMF, the above equation needs to be solved only in those regions of $x_0$ where

the profile function is non-negligible. This, however, corresponds to the resonance zone, where the

SA assumes that all macro-variables (except for v) are spatially constant. In this spirit, when

neglecting the spatial derivative in the above equation, the Sobolev-limit can be easily obtained!

We will show this here for the case of one purely absorbing line (no cont.) at frequency $\tilde{\nu}$ (and positive $\mu$),

the generalization is left as an exercise for the reader  (or: see Lucy 1971, Puls 1991)  $\Rightarrow$

$$-P(r,\mu)\frac{\partial I_0^{+}(z,p,x_0)}{\partial x_0} = -\chi_0(r,x_0)I_0^{+}(z,p,x_0) \quad \text{where } (z,r,\mu) \text{ refer to the resonance zone}$$

$$\ln\left[I_0^{+}(z,p,x_0)/I_0^{\text{inc}}(z,p,x_{0,B})\right] = \frac{\overline{\chi}_L(r)}{\Delta\nu_{\infty}P(r,\mu)}\int_{x_{0,B}}^{x_0}\phi(x)\mathrm{d}x \qquad [\Delta\nu_{\infty} \text{ since frequency } x_0 \text{ and not } \nu_0]$$

$$I_0^{+}(z,p,x_0) = I_0^{\text{inc}}(z,p,x_{0,B}) \exp\left[-\tau_S(r,\mu)\,\Phi(x_0)\right],$$

q.e.d. [compare with slide 28, and note that the above solution is already evaluated in the resonance zone]

… as for (quasi-isotropic) continuum (cf. slide 18):

METHOD 1 (formal solution for *I*): use 'only' the discretized CMF-RTE for Feautrier variables, $u=1/2(I^{+}+I^{-})$ and $v=1/2(I^{+}-I^{-})$. In p-z geometry:

$$\frac{\partial u^0}{\partial z} - P\frac{\partial v^0}{\partial x_0} = -\chi_0 v^0$$

$$\frac{\partial v^0}{\partial z} - P\frac{\partial u^0}{\partial x_0} = \chi_0(S_0 - u^0)$$

$x_0$ CMF-frequency in Doppler-units w.r.t. $v_\infty$

$$P(r,\mu) = \frac{d(\mu v/v_\infty)}{dz} = \left( \mu^2 \frac{dv/v_\infty}{dr} + (1-\mu^2)\frac{v/v_\infty}{r} \right);$$

don't confuse Feautrier v with velocity v!

- two coupled first order PDEs
- (almost) all variables are in the CMF, and depend on *z* (or *r*) and $x_0$.
- boundary values as before (slide 18), plus 'blue-wing' boundary condition at bluest frequency, from pure continuum transport. Attention: if integration over large frequency range, care needs to be taken in the formulation of the outer boundary condition when optically thick; otherwise numerical artefacts created and transported through the grid!
- approximate lambda operator (ALO) can be calculated in parallel (see slide 58).
- discretization:
    - either using fully implicit scheme; 2nd order in space, 1st order in frequency: unconditionally stable (Mihalas et al. 1975)
    - or semi-implicit (Crank-Nicholson) scheme; higher accuracy, since 2nd order in frequency: if used in the formulation by Hamann (1981) [and NOT in the formulation by Mihalas et al. 1975], unconditionally stable as well (according to the author)

METHOD2 (variable Eddington factors): use CMF moments equations to obtain moments of radiation field (in the CMF). Contrasted to observer's frame equations (slide 16/19), 3rd moment (of specific intensity), $N_\nu^0$, present.

$$\frac{1}{r^2}\frac{\partial\left(r^2 H_\nu^0\right)}{\partial r} - \frac{\nu_0}{c}\left[\frac{v}{r}\frac{\partial(J_\nu^0 - K_\nu^0)}{\partial \nu_0} + \frac{dv}{dr}\frac{\partial K_\nu^0}{\partial \nu_0}\right] = \eta_0(\nu_0) - \chi_0(\nu_0)J_\nu^0$$

$$\frac{\partial K_\nu^0}{\partial r} + \frac{3K_\nu^0 - J_\nu^0}{r} - \frac{\nu_0}{c}\left[\frac{v}{r}\frac{\partial(H_\nu^0 - N_\nu^0)}{\partial \nu_0} + \frac{dv}{dr}\frac{\partial N_\nu^0}{\partial \nu_0}\right] = -\chi_0(\nu_0)H_\nu^0$$

By means of the sphericality factor $q_\nu$ from slide 19 and the Eddington factors $f_\nu^0 = \dfrac{K_\nu^0}{J_\nu^0}$ and $g_\nu^0 = \dfrac{N_\nu^0}{H_\nu^0}$

(calculated from the formal solution)

we obtain again a coupled system of 1st order PDEs for $r^2 J_\nu^0$ and $r^2 H_\nu^0$ that can be solved by discretization:

$$-\frac{\partial\left(r^2 H_\nu^0\right)}{\partial r} + \frac{\nu_0}{c}\left[\frac{dv}{dr} - \frac{v}{r}\right]\frac{\partial\left(f_\nu^0 r^2 J_\nu^0\right)}{\partial \nu_0} + \frac{\nu_0}{c}\frac{v}{r}\frac{\partial\left(r^2 J_\nu^0\right)}{\partial \nu_0} = \chi_0(\nu_0)\left(r^2 J_\nu^0 - r^2 S_\nu^0\right)$$

$$-\frac{\partial\left(q_\nu f_\nu^0 r^2 J_\nu^0\right)}{q_\nu \partial r} + \frac{\nu_0}{c}\left[\frac{dv}{dr} - \frac{v}{r}\right]\frac{\partial\left(g_\nu^0 r^2 H_\nu^0\right)}{\partial \nu_0} + \frac{\nu_0}{c}\frac{v}{r}\frac{\partial\left(r^2 H_\nu^0\right)}{\partial \nu_0} = \chi_0(\nu_0)\,r^2 H_\nu^0$$

In case, use Rybicki scheme if source function can be separated into scattering and true absorption/emission components.

hot supergiant (Teff = 45,000 K), dense wind          "cool" dwarf (Teff = 28,000 K), moderate wind
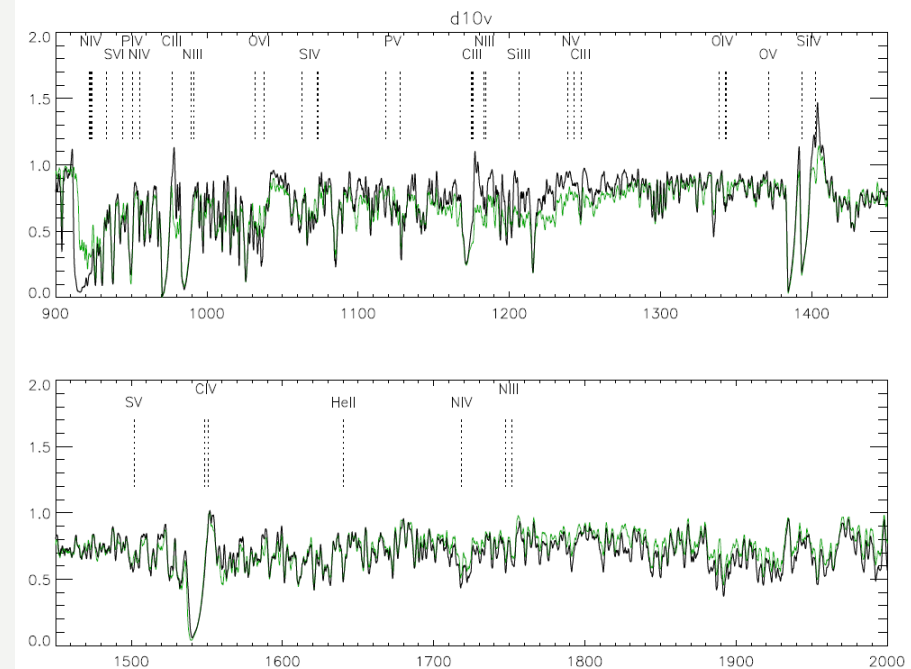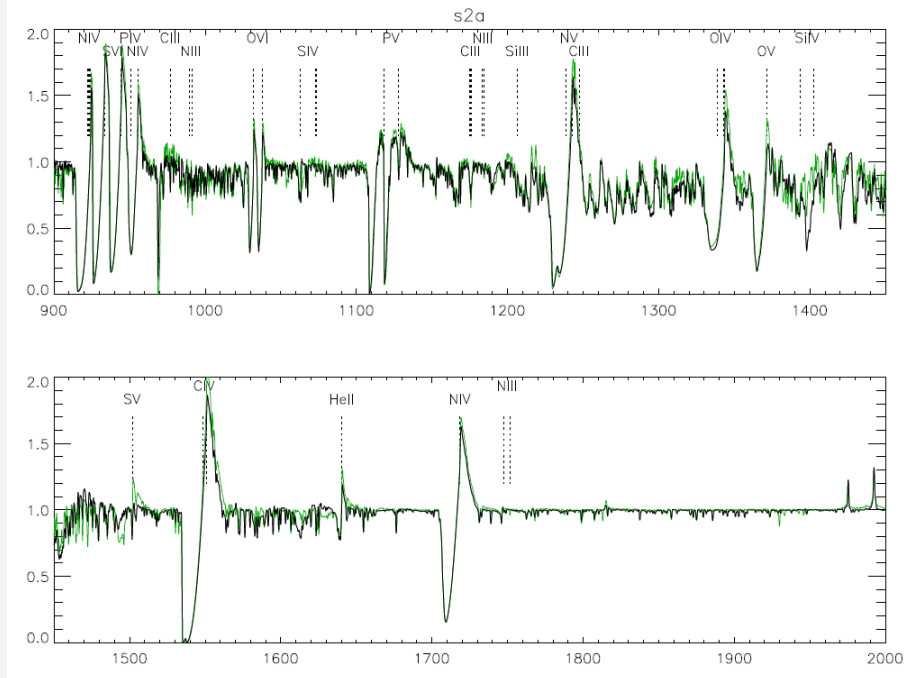


Theoretical UV spectra (900 – 2000 Å) for a hot supergiant (Teff = 45,000 K, log g = 3.8) with a dense wind **(left)**, and for a "cool" dwarf (Teff = 28,000 K, log g = 3.9) **(right)**, as synthesized by FASTWIND v11 (black) and CMFGEN (green). The model spectra for the supergiant were convolved with v sini = 80 km/s, whilst for the dwarf model v sini = 200 km/s was used, to allow for an easy comparison. Line identifiers for "light" ions provided.
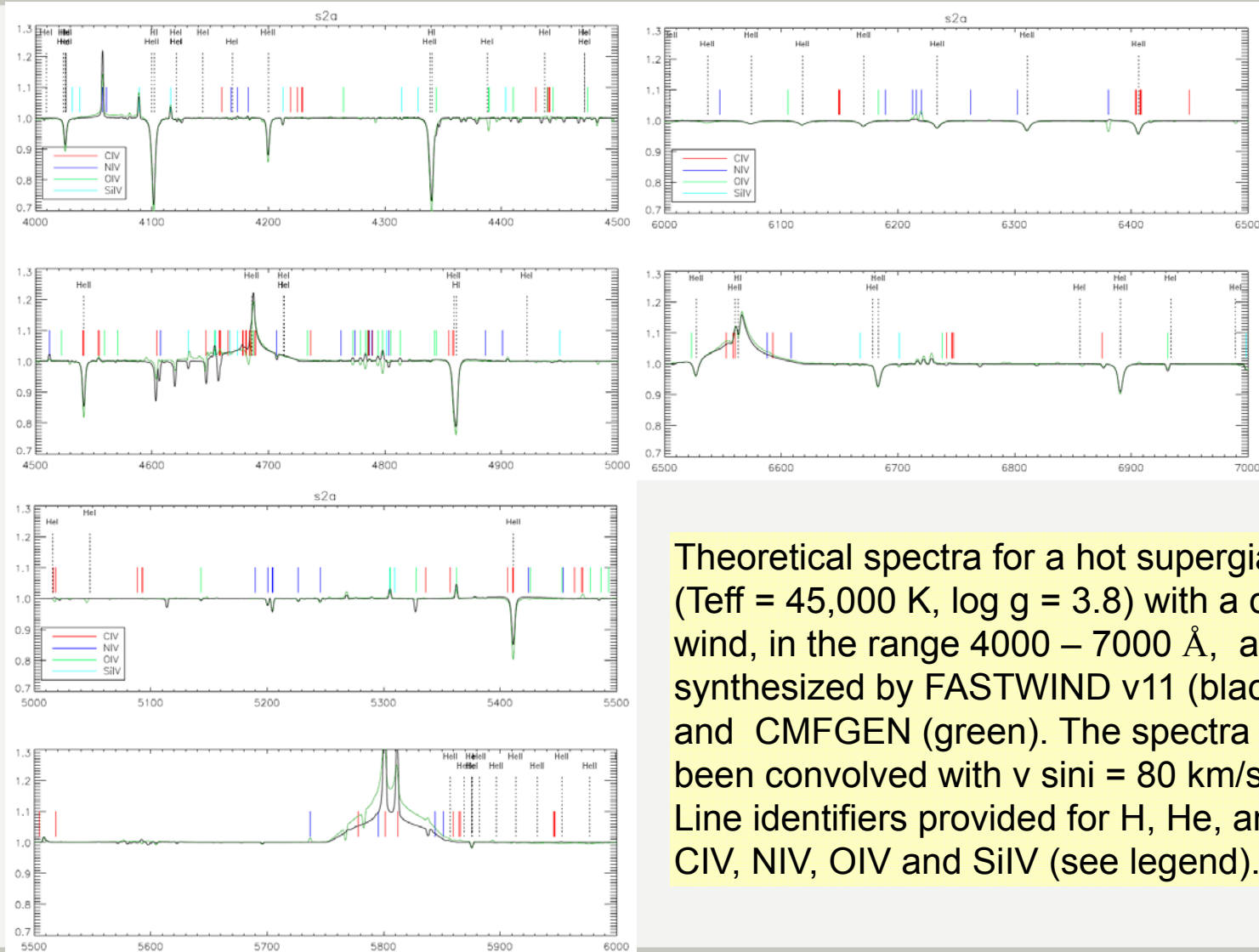
Theoretical spectra for a hot supergiant (Teff = 45,000 K, log g = 3.8) with a dense wind, in the range 4000 – 7000 Å, as synthesized by FASTWIND v11 (black) and CMFGEN (green). The spectra have been convolved with v sini = 80 km/s. Line identifiers provided for H, He, and CIV, NIV, OIV and SiIV (see legend).

To calculate the radiative acceleration, in the observer's frame we would need to evaluate (see slide 16)

$$\rho \mathbf{g}_{\text{rad}} = \frac{1}{c} \int d\nu \oint \left( \chi_\nu \left( \nu(1 - \mu v/c) \right) I_\nu(\mu) - \eta_\nu \left( \nu(1 - \mu v/c) \right) \right) \mathbf{n} d\Omega,$$

since the (line-) opacities and emissivities are angle-dependent when a velocity field is present.

Because of the isotropy of $\chi_\nu$ and $\eta_\nu$ in the comoving frame, however, this expression becomes considerably simplified when evaluated in the CMF,

$$\mathbf{g}_{\text{rad}}^0 = \frac{4\pi}{c\rho} \int d\nu \, \chi_\nu^0 H_\nu^0, \quad \text{since} \oint \chi_\nu^0 I_0(\mu, \nu_0) \mathbf{n} d\Omega = \chi_\nu^0 4\pi H_\nu^0 \quad \text{and} \quad \oint \eta_\nu^0 \mathbf{n} d\Omega = 0$$

[Remember as well that also in the "standard" SA, the contribution due to emission cancels, because of the fore-aft symmetry of $\tau_S$. Source-function gradients do change this picture though, e.g. Puls & Hummer 1988]

Interestingly (and fortunately) one can show (e.g., Mihalas, "Stellar atmospheres", 2nd edition, Chap. 15.3) that this expression is not only valid when used within the fluid frame (=CMF) equations of motion, but also, to order $(v/c)$, in the corresponding inertial frame formulation. Namely, when the moments of the radiation field contained in the coupled matter-radiation equation of motion are expressed in terms of their CMF-counterparts, and if the CMF moments equations (see below) are used, a delicate cancellation of terms ensures that also in the inertial frame the above expression for $\mathbf{g}_{\text{rad}}^0 \overset{O(v/c)}{\rightarrow} \mathbf{g}_{\text{rad}}$ can be used for the radiative acceleration.
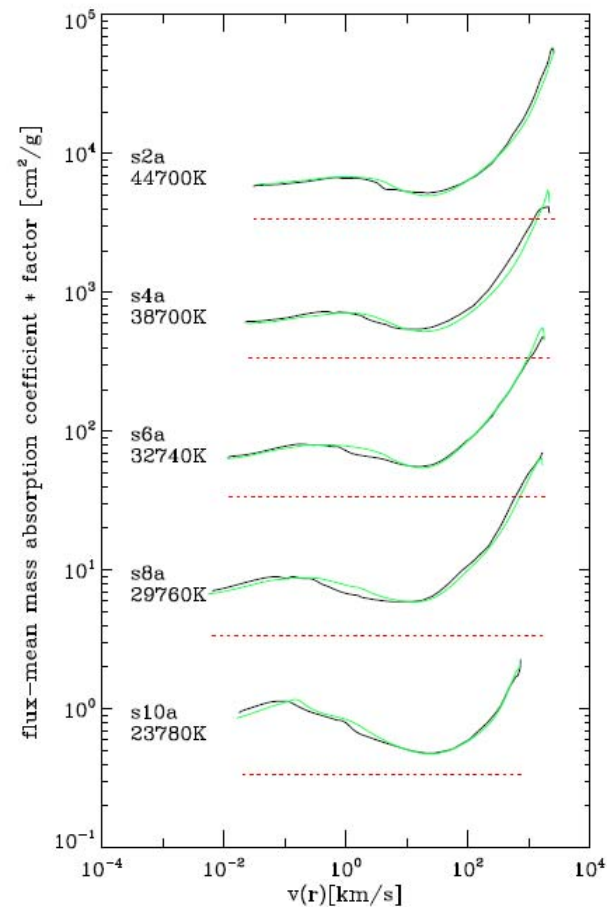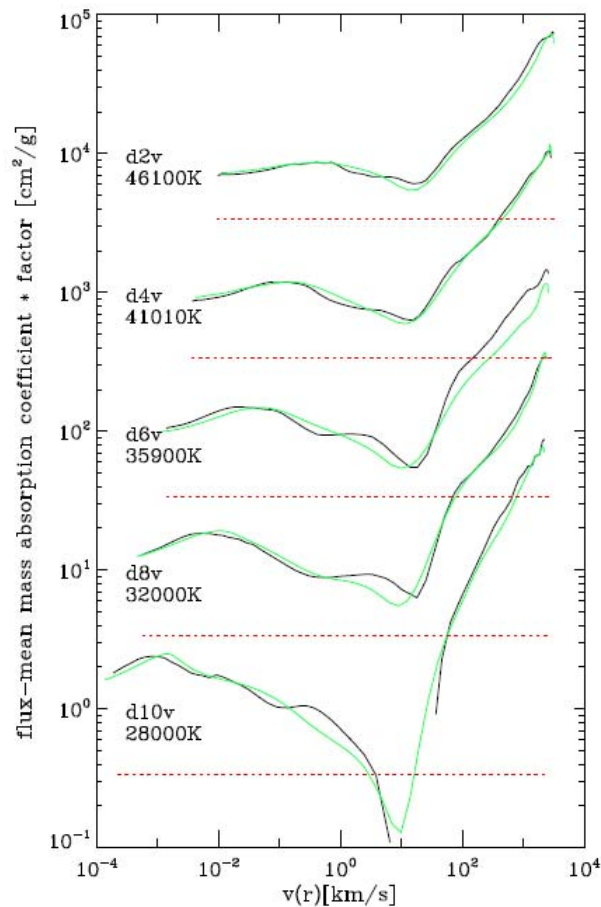
Comparison of flux-mean mass absorption coefficient, a quantity directly proportional to the total radiative acceleration, for dwarf (left) and supergiant models (right) from FASTWIND v11 (black) and CMFGEN (green).
The red lines indicate the corresponding "acceleration" by pure Thomson scattering. For convenience, all curves (but the lowest ones) have been shifted by multiples of 1 dex.

- Not directly related to radiative transfer, but important if NLTE treatment required as in the case of hot stars, where radiative rates dominate over collisional ones in the line-forming region, due to strong radiation field (and low densities in stellar wind).
- NLTE: coupling between radiation field and occupation numbers via rate equations
- two methods to obtain consistent solution
    - complete linearization (Auer & Mihalas 1969), used, e.g., in CMFGEN (Appendix A)
    - (Accelerated) Lambda iteration (Werner & Husfeld 1985), used, e.g., in PoWR, WM-basic, FASTWIND (Appendix A)
- ALI: easier to program and faster per iteration step, but often more iterations

**BASIC IDEA:** Lambda-iteration
- start with guess values (e.g., LTE or simplified NLTE) for occupation numbers
- calculate opacities and source-functions
- perform RT, calculate mean intensities and scattering integrals
- solve rate equations involving $J_\nu$ and $\overline{J}$, i.e., calculate new occupation numbers

**iteration**

**PROBLEM(s):**
- very slow convergence for optically thick, scattering dominated processes, if at all
- difficulty to define appropriate convergence criterion
- can be shown: during each iteration, information is propagated only over $\Delta\tau_\nu \approx 1$

Simple example: purely scattering line (e.g., UV-resonance line) in Sobolev approach

i) $S = \bar{J}$   most simple "rate equation" $\left(\text{e.g., from two-level atom without collisions}\right)$

ii) $\bar{J} = (1-\beta)S + \beta_c I_{core}$   "formal solution" (see slide 30 , Sobolev solution for line-transfer in optically thin continuum)

Let's assume that the opacities are known and remain constant over the iteration (not too wrong for resonance lines)

**A :** In this case, it's possible to obtain a consistent analytic solution, using (i) and (ii) in parallel

$$S = (1-\beta)S + \beta_c I_{core} \;\Rightarrow\; \boxed{S = \frac{\beta_c I_{core}}{\beta}}$$   (balance between irradiation and escape)

**B :** alternatively, we use the Lambda iteration

We start with a guess value for the source-function, $S^0$, and calculate the scattering integral, $\bar{J}^0$, using ii)

Then we determine a new iterate for the source function, $S^1$, using i)

$$\Rightarrow S^1 = (1-\beta)S^0 + \beta_c I_{core}. \qquad \text{Generally,}$$

$$\left.\begin{array}{l} S^n = (1-\beta)S^{n-1} + \beta_c I_{core} \\ S^{n-1} = (1-\beta)S^{n-2} + \beta_c I_{core} \end{array}\right\} \quad S^n - S^{n-1} := \boxed{\Delta S^n = (1-\beta)\Delta S^{n-1}}$$

and for optically thick lines $(\beta \to \frac{1}{\tau_S})$, $\beta \ll 1$, $\Delta S^n \approx \Delta S^{n-1}$, no reasonable convergence criterium can be defined ...

When do we consider the solution as converged???

... and how does the direct solution (A) and the iterated solution (B) compare?

Let's investigate the limiting value for $n \to \infty$

$$S^n = (1-\beta)S^{n-1} + \beta_c I_{\text{core}} = (1-\beta)\left[(1-\beta)S^{n-2} + \beta_c I_{\text{core}}\right] + \beta_c I_{\text{core}}$$

$$= \ ... \ = (1-\beta)^n S^o + \beta_c I_{\text{core}}\left[(1-\beta)^{n-1} + (1-\beta)^{n-2} + ... + 1\right]$$

With $\displaystyle\sum_{i=0}^{n-1} q^i = \frac{1-q^n}{1-q}$ we thus find

$$S^n = (1-\beta)^n S^0 + \beta_c I_{\text{core}}\frac{1-(1-\beta)^n}{\beta} \quad \xrightarrow{n\to\infty} \quad \frac{\beta_c I_{\text{core}}}{\beta},$$

i.e., indeed the Lambda-iterated solution (from B) converges (very slowly) to the correct one (from A),

(and becomes independent from the start value)

How many iteration steps would be required?

For $\beta \ll 1$, we can approximate $(1-\beta)^n \approx (1-n\beta)$, and to ensure convergence, we must have $(1-n\beta) \to 0$,

i.e., $n \approx \dfrac{1}{\beta} \to \tau_S$

Thus, we would need the same number of iterations as the size of $\tau_S$, which

(i) can be very large for resonance lines, $n \approx \tau_S$ up to $O(10^5 ... 10^6)$, and

(ii) shows that indeed, per iteration step, information corresponding to only $\Delta\tau = 1$ is propagated

General problem: For a consistent solution, we need

$$S^n \overset{\overset{\text{via rate equations}}{\frown}}{=} f(J^n) = f\left( \overbrace{\Lambda\left[ S^n \right]}^{\text{formal solution}} \right),$$

which is a non-linear and (except for the Sobolev-case) non local problem.

In contrast, the lambda iteration provides us with

$$S^n = f(J^{n-1}) = f(\Lambda\left[ S^{n-1} \right]),$$

which displays the well-known convergence problems.

In the following, we consider continuum ($J$) and line-problems ($\bar{J}$) in parallel.

Generalization of results for continuum quantities to line conditions is straightforward,

by solving for all line-frequencies and integrating over the profile-function.

For values on a 1-D spatial grid (with $N$ grid-points), we may write

$$\mathbf{J} = \Lambda[\mathbf{S}] = \mathbf{\Lambda} \cdot \mathbf{S} + \mathbf{\Phi},$$

Thus, $\Lambda$ is an affine operator (linear transformation + displacement), due to boundary conditions,

$\mathbf{J}$, $\mathbf{S}$, and $\mathbf{\Phi}$ are vectors of length $N$, and $\mathbf{\Lambda}$ is a matrix with $N \times N$ elements.

$\mathbf{\Phi}$ corresponds to the boundary conditions $\left( \mathbf{J}(\mathbf{S} = \mathbf{0}) \right)$.

If required, the elements $\Lambda_{ij}$ and $\Phi_i$ could be derived (in 1-D) from $N + 1$ formal solutions with $\mathbf{S} = \mathbf{0}$, $\mathbf{S} = \mathbf{e_1}$, ..., $\mathbf{S} = \mathbf{e_N}$

ALI bases on the idea of operator-splitting (e.g., Cannon 1973), namely to split

$$\Lambda = \Lambda^{A} + \left( \Lambda - \Lambda^{A} \right)$$

the lambda-operator into an approximate operator (which should be easily invertible), and a rest part $\left[ \text{similar to the Jacobi iteration in boundary value problems} \right]$. Then we can approximate

$$\mathbf{J^n} \approx \Lambda^{A}\left[ \mathbf{S^n} \right] + \left( \Lambda - \Lambda^{A} \right)\left[ \mathbf{S^{n-1}} \right]$$

This is the "trick", since now we have a relation between $\mathbf{J^n}$ and $\mathbf{S^n}$, and not only between $\mathbf{J^{n-1}}$ and $\mathbf{S^{n-1}}$

where identity is obtained for $n \to \infty$, when $\mathrm{S^{n-1}} \to \mathrm{S^n}$.

Also the approximate lambda operator (ALO), $\Lambda^{A}$, needs to be of affine type, i.e., $\Lambda^{A}\left[ \mathbf{S} \right] = \Lambda^{*} \cdot \mathbf{S} + \mathbf{\Phi}^{*}$, but even then

$$\mathbf{J^n} = \left[ \Lambda^{*} \cdot \mathbf{S^n} + \mathbf{\Phi}^{*} \right] + \mathbf{J^{n-1}} - \left[ \Lambda^{*} \cdot \mathbf{S^{n-1}} + \mathbf{\Phi}^{*} \right], \ \text{i.e.,} \ \boxed{\mathbf{J^n} = \Lambda^{*} \cdot \mathbf{S^n} + \Delta \mathbf{J}^{n-1}} \ \text{with} \ \Delta \mathbf{J}^{n-1} = \mathbf{J^{n-1}} - \Lambda^{*} \cdot \mathbf{S^{n-1}},$$

only the linear part of the ALO, $\Lambda^{*}$, is required, assuming that $\mathbf{\Phi}^{*}$ remains constant over the iteration.

Note that $\Delta \mathbf{J}^{n-1}$ depends only on $\mathbf{S^{n-1}}$, and can be calculated from the formal solution for $\mathbf{J^{n-1}}$ (and specified $\Lambda^{*}$).

Now let's adopt a continuum with scattering, or -- again -- a two-level atom,

$$\mathbf{S} = \xi\mathbf{J} + \psi$$

where $\xi$ is a diagonal matrix (containing the scattering fractions $0 \le \xi_{ii} \le 1$)

and $\psi$ a vector (containing the Planck-functions). Then,

$$\mathbf{S^n} = \xi\left(\Lambda^*\mathbf{S^n} + \Delta\mathbf{J^{n-1}}\right) + \psi,$$

and we obtain an *explicit* expression for $\mathbf{S^n}$,

$$\mathbf{S^n} = \left(1 - \xi\Lambda^*\right)^{-1}\left(\xi\Delta\mathbf{J^{n-1}} + \psi\right) = \left(1 - \xi\Lambda^*\right)^{-1}\left(\xi(\Lambda - \Lambda^*)\mathbf{S^{n-1}} + \psi\right)$$

ALI scheme for "simple" source-functions

With $\Delta\mathbf{S^n} := \mathbf{S^n} - \mathbf{S^\infty}$ (deviation from the "true" source function $\mathbf{S^\infty}$, contrasted to the def. on slide 53), we thus find (after few algebraic manipulations)

$$\Delta\mathbf{S^n} = \mathbf{A}\Delta\mathbf{S^{n-1}}$$ with "amplification matrix" $\mathbf{A} = \left(1 - \xi\Lambda^*\right)^{-1}\left(\xi(\Lambda - \Lambda^*)\right).$

One can show that under typical conditions $\mathbf{A}$ has a complete set of real and orthogonal eigenvectors and real eigenvalues $\lambda$ (e.g., Puls & Herrero 1988). Expanding $\Delta\mathbf{S}$ in terms of these eigenvectors, for large $n$ we obtain $\boxed{\Delta\mathbf{S^n} \approx \lambda_{max}^n \Delta\mathbf{S^0}}$ ,

where $\lambda_{max}$ is the maximum eigenvalue (when ordered according to absolute values).

Thus, the ALI scheme converges if $|\lambda_{max}| < 1,$ and else diverges.

For static problems, Olson, Auer & Buchler (1986) showed that indeed

$$\left|\lambda_{\max}\right| < 1 \quad \text{if} \quad \mathbf{\Lambda}^* = \text{diag}\,(\mathbf{\Lambda}).$$

A very fast calculation of the corresponding $\mathbf{\Lambda}^*$ has been provided by Rybicki & Hummer (1991, Appendix).
For the case of CMF line transfer, Puls (1991) developed an appropriate, purely local ALO.
NOTE 1: since the CMF line transfer has an essentially local character in rapidly expanding atmospheres
(taking place only in the narrow resonance zone), a local ALO is sufficient when solving for the rate equations
under such conditions
NOTE 2: for local ALOs, an overestimation of the exact diagonal leads to divergence in most cases

For non-local ALOs and more sophisticated iteration schemes (e.g., required in multi-D calculations),
see Trujillo Bueno & Fabiani Bendicho (1995) and references therein. See also Hennicker et al. (2017 and poster).

Comparison between ALI-scheme and Sobolev approach (line case)
Assuming a local ALO, for each depth point we have the correspondance

ALI: $\quad \bar{J}^n = \quad \Lambda^* S^n \quad + \quad \underbrace{\Delta\bar{J}^{n-1}}_{\bar{J}^{n-1}-\Lambda^* S^{n-1}}$

Sobolev: $\bar{J}^n = (1-\beta)S^n \quad + \quad \beta_c I_{\text{core}}$

$\left.\begin{array}{c}\\\\\\\end{array}\right\} \Lambda^* \triangleq (1-\beta), \ \text{and} \ \Delta\bar{J}^{n-1} \triangleq \beta_c I_{\text{core}}$
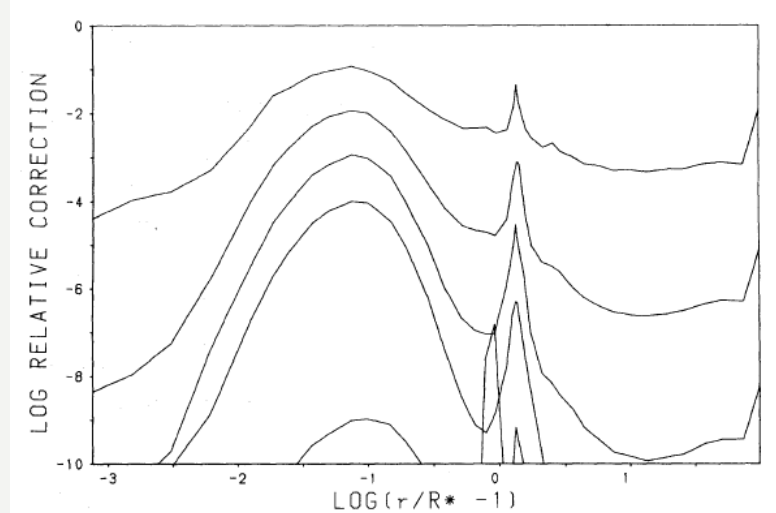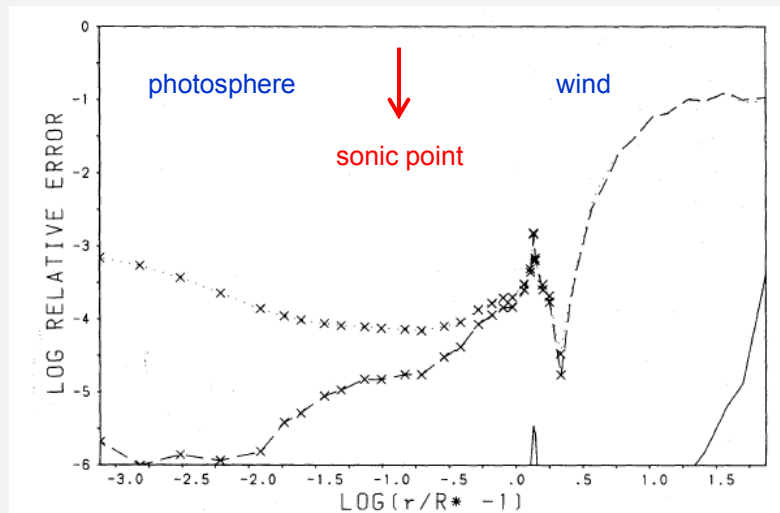
solid: deviation between exact diagonal and Λ*
dotted: deviation between exact diag. and (1-β)
Note: 1-β overestimates the excact diagonal
in most regions, thus cannot be used as ALO

relative corrections for subsequent iterations

ALO, Λ*, and ALI-cycle for a line source function calculated in the CMF, using the ALO from Puls (1991). The displayed example refers to a strong, purely scattering line.

Net line rate (in rate equations) $Z_{ul}$, for a transition with upper and lower levels $u, l$,

and corresponding occupation numbers $n_u, n_l$

$$Z_{ul} = n_u A_{ul} \left( 1 - \frac{\bar{J}}{S} \right) \quad \text{with Einstein-coefficient (for spontaneous emission) } A_{ul}$$

$$S = \frac{n_u A_{ul}}{n_l B_{lu} - n_u B_{ul}} \quad \text{with Einstein coefficients for absorption and induced emission, } B_{lu} \text{ and } B_{ul}$$

**1. Without ALI, applying conventional lambda iteration**

Rate equations for $S^n$ calculated using $\bar{J}^{n-1}$

$$\Rightarrow \frac{\bar{J}^{n-1}}{S^n} = \bar{J}^{n-1} \left( \frac{n_l B_{lu} - n_u B_{ul}}{n_u A_{ul}} \right)$$

$$\Rightarrow Z_{ul} = n_u \underbrace{\left( A_{ul} + B_{ul} \bar{J}^{n-1} \right)}_{\text{downward line rate}} - n_l \underbrace{B_{lu} \bar{J}^{n-1}}_{\text{upward line rate}}$$

**Comparison:**

$$\left. \begin{array}{l} A_{ul} \rightarrow A_{ul}(1 - \Lambda^*) \\ B_{ul} \bar{J}^{n-1} \rightarrow B_{ul} \Delta \bar{J}^{n-1} \\ B_{lu} \bar{J}^{n-1} \rightarrow B_{lu} \Delta \bar{J}^{n-1} \end{array} \right\} \text{all rates become smaller:}$$

inefficient part (optically thick line core, where upward and downward rates are equal)

analytically cancelled, only efficient part (optically thin wings) survives;

denoted as "preconditioning" by Rybicki & Hummer 1991; sometimes also called "effective" or "reduced" rates

**2. With ALI and local ALO**

Rate equations for $S^n$ calculated using $\bar{J}^n = \Lambda^* S^n + \Delta \bar{J}^{n-1}$

$$\frac{\bar{J}^n}{S^n} = \Lambda^* + \frac{\Delta \bar{J}^{n-1}}{S^n}$$

$$\Rightarrow Z_{ul} = n_u A_{ul} \left( 1 - \Lambda^* - \frac{\Delta \bar{J}^{n-1}}{S^n} \right) =$$

$$= n_u \underbrace{\left( A_{ul}(1 - \Lambda^*) + B_{ul} \Delta \bar{J}^{n-1} \right)}_{\text{downward line rate}} - n_l \underbrace{B_{lu} \Delta \bar{J}^{n-1}}_{\text{upward line rate}}$$

inserting the scattering integral derived by means of the Sobolev approximation,

$$Z_{ul} = n_u \left( A_{ul} + B_{ul}\bar{J} \right) - n_l B_{lu}\bar{J} = n_u \left( A_{ul} + B_{ul}\left[ (1-\beta)S + \beta_c I_{core} \right] \right) - n_l B_{lu}\left[ (1-\beta)S + \beta_c I_{core} \right] = \dots$$
$$= n_u \left( A_{ul}\beta + B_{ul}\beta_c I_{core} \right) - n_l B_{lu}\beta_c I_{core}.$$

Also here the contribution from the optically thick core cancels analytically.

By comparing with the analogous result using ALI, we again find the correspondance (see slide 58 )

$$\Lambda^* \triangleq (1-\beta), \quad \text{and} \quad \Delta\bar{J}^{n-1} \triangleq \beta_c I_{core}$$

If one would use the Sobolev approximation with continuum (slide 38), this correspondance would read

$$\Lambda^* \triangleq (1-\beta-\bar{U}), \quad \text{and} \quad \Delta\bar{J}^{n-1} \triangleq \overline{\beta_c(r)I_{inc}} + \bar{U}S_c$$

Multitude of additional issues, not treated here due to time constraints;
marked in red if directly related to specific RT problems.

❑ temperature structure: radiative equilibrium vs. thermal electron balance

❑ energy equation, adiabatic expansion and cooling in the outermost wind

❑ the line-driven instability (LDI), and impact of diffuse radiation field

❑ inhomogeneous winds, shocks, and X-ray emission

❑ examples/applications
  ❑ UV P-Cygni line formation
  ❑ supersonic "micro-turbulence" vs. non-monotonic v-fields
  ❑ supersonic macro-turbulence
  ❑ (quasi-) recombination lines
  ❑ optical-depth invariants → scaling relations
  ❑ $H_\alpha$ in O-stars and AB-supergiants
  ❑ impact of wind on weaker lines/NIII 4640
  ❑ IR/radio excess
  ❑ IR-lines: inverted levels (or close to inversion)
  ❑ X-rays: impact on resonance lines/"superionization"
  ❑ emission lines in WRs

❑ wind inhomogeneities/clumping
- ❑ micro- and macro-clumping, porosity
- ❑ clumping in RTE
- ❑ $H_\alpha$ vs. HeII4686
- ❑ velocity-porosity
- ❑ clumping – coupling with rate equations

❑ outlook:
- ❑ 2/3-D problems/formulation
- ❑ time-dependence, relativistic treatment
- ❑ non-radial line-forces (e.g., in rotating winds)
- ❑ polarization (linear, circular -> B-fields)

# Appendix A
# NLTE model atmosphere codes
# for hot stars

| | Detail/Surf. (1) | TLUSTY (2) | CMFGEN (3) | FASTWIND (4) | Phoenix (5) | PoWR (6) | WM-basic (7) |
|---|---|---|---|---|---|---|---|
| geometry | codes described in (1) Giddings (1981), Butler & Giddings (1985); (2) Hubeny (1998); (3) Hillier & Miller (1998); (4) Puls et al. (2005); ); (5) Hauschildt (1992); (6) Gräfener et al. (2002); (7) Pauldrach et al. (2001) | | | | | | |
| blanketing | | | | | | | |
| radiative line transfer | | | | | | | |
| | color coding of following Table | | | | | | |
| temperature structure | optimum treatment (at present state of the art) | | | | | | |
| photosphere | | | | | | | |
| diagnostic range | | | | | | | |
| major application | less than optimum (but usually faster) | | | | | | |
| comments | | | | | | | |
| execution time | | | | | | | |

# NLTE model atmosphere codes for hot stars

| | Detail/Surf. (Butler) | TLUSTY (Hubeny) | CMFGEN (Hillier) | Fastwind (Puls) | Phoenix (Hauschildt) | PoWR (Hamann) | WM-basic (Pauldrach) |
|---|---|---|---|---|---|---|---|
| geometry | plane-parallel | plane-parallel | spherical | spherical | spherical/ plane-parallel | spherical | spherical |
| blanketing | LTE | yes | yes | approx. | yes | yes | yes |
| radiative line transfer | observer's frame | observer's frame | CMF | CMF/ Sobolev | CMF/ obs.frame | CMF | Sobolev |
| temperature structure | radiative equilibrium | radiative equilibrium | radiative equilibrium | e⁻ therm. balance | radiative equilibrium | radiative equilibrium | e⁻ therm. balance |
| photosphere | yes | yes | yes | yes | yes | yes | approx. |
| diagnostic range | no limitation | no limitation | no limitation | optical/IR | no limitation | no limitation | UV |
| major application | hot stars with negl. winds | hot stars with negl. winds | OB(A)-stars, WRs, SNe | OB-stars, early A-sgs | stars below 10kK, SNe | WRs, O-stars | hot stars with dense winds, ion. fluxes, SNe |
| comments | no wind | no wind | start model required | expl./backgr. elements | molecules incl. / no clumping | | no clumping |
| execution time | few minutes | hour(s) | hours | 0.25 - 0.5 h (v10) 1.5-2 h (v11) | hours | hours | 1 to 2 h |

Appendix B
Further comments on the
line-profile function

## 1. DEPTH-DEPENDENT THERMAL SPEEDS

To avoid a depth-dependence of the frequency grid when measuring frequencies in
(depth-dependent) Doppler-units, one uses a FIDUCIAL thermal speed, $v_{th}^*$,

$$x = \frac{\nu - \tilde{\nu}}{\Delta\nu_D^*} \quad \text{with} \quad \Delta\nu_D^* = \frac{\tilde{\nu}v_{th}^*}{c}.$$

Let $\delta(r) = \dfrac{\Delta\nu_D(r)}{\Delta\nu_D^*} = \dfrac{v_{th}(r)}{v_{th}^*}$, then $\dfrac{\nu - \tilde{\nu} - \mu v(r)\tilde{\nu}/c}{\Delta\nu_D(r)} = \dfrac{x - \mu v'(r)}{\delta(r)}$, again with $v'(r) = \dfrac{v(r)}{v_{th}^*}$

In this notation,

$$\phi_\nu(x_{CMF},r) = \phi_\nu(x - \mu v', r) = \frac{1}{\Delta\nu_D^*\delta(r)\sqrt{\pi}}\exp\left[-\left(\frac{x - \mu v'(r)}{\delta(r)}\right)^2\right],$$

with units "per frequency" $[s]$, or alternatively

$$\chi_\nu(x_{CMF},r) = \frac{\bar{\chi}_L(r)}{\Delta\nu_D^*}\,\phi(x_{CMF},r), \quad \text{with dimensionless}$$

$$\phi(x_{CMF},r) = \frac{1}{\delta(r)\sqrt{\pi}}\exp\left[-\left(\frac{x - \mu v'(r)}{\delta(r)}\right)^2\right], \quad \text{and} \quad \frac{\bar{\chi}_L(r)}{\Delta\nu_D^*} = \frac{\bar{\chi}_L(r)\tilde{\lambda}}{v_{th}^*}.$$

## Appendix B
## Further comments on the
## line-profile function

LMU  USM

2. INTEGRALS INVOLVING THE PROFILE FUNCTION: Which normalization to use?

(i) spatial integrals of type $\int \chi(\nu_{\text{CMF}}, r) f_\nu(r)\, dr \;\;\rightarrow\;\; \int \dfrac{\overline{\chi}_{\text{L}}(r)}{\Delta \nu_{\text{D}}}\, \phi(x_{\text{CMF}}, r) f_\nu(r)\, dr$

[e.g., optical depth if $f_\nu(r) = 1$]

(ii) frequency integrals of type $\int f_\nu(r)\, \phi(\nu_{\text{CMF}}, r)\, d\nu \;\;\rightarrow\;\; \int f(\nu(x), r)\, \phi(x_{\text{CMF}}, r)\, dx$

[e.g., scattering integrals, if $f_\nu(r) = J_\nu(r)$]

(iii) frequency integrals of type $\int \chi(\nu_{\text{CMF}}, r) f_\nu(r)\, d\nu \;\;\rightarrow\;\; \overline{\chi}_{\text{L}}(r) \int f(\nu(x), r)\, \phi(x_{\text{CMF}}, r)\, dx$

[e.g., in the context of $g_{\text{rad}}(r)$, see <span>slide 34</span>]

with $\phi(\nu_{\text{CMF}}, r) = \dfrac{\phi(x_{\text{CMF}}, r)}{\Delta \nu_{\text{D}}}$, i.e., $\phi(\nu_{\text{CMF}}, r)\, d\nu = \phi(x_{\text{CMF}}, r)\, dx$, and

$\phi(\nu_{\text{CMF}}, r) = \phi_\nu(x_{\text{CMF}}, r)$ normalized w.r.t. frequency, $\phi(x_{\text{CMF}}, r)$ normalized w.r.t. $x$.

## References

Auer, L. H., and Mihalas, D. 1969. Brackett-Alpha Emission in Non-Lte Model Stellar Atmospheres. *ApJ*, **156**(June), L151.

Cannon, C. J. 1973. Frequency-Quadrature Perturbations in Radiative-Transfer Theory. *ApJ*, **185**(Oct.), 621–630.

Castor, J. I. 1972. Radiative Transfer in Spherically Symmetric Flows. *ApJ*, **178**(Dec.), 779–792.

Castor, J. I., Abbott, D. C., and Klein, R. I. 1975. Radiation-driven winds of Of stars. *ApJ*, **195**(Jan.), 157–174.

Castor, J. L. 1974. On the force associated with absorption of spectral line radiation. *MNRAS*, **169**(Nov.), 279–306.

Friend, D. B., and Castor, J. I. 1983. Stellar winds driven by multiline scattering. *ApJ*, **272**(Sept.), 259–272.

Gabler, R., Gabler, A., Kudritzki, R. P., Puls, J., and Pauldrach, A. 1989. Unified NLTE model atmospheres including spherical extension and stellar winds - Method and first results. *A&A*, **226**(Dec.), 162–182.

Giddings, J. R. 1981. Ph.D. thesis, , University of London, (1981).

Hamann, W.-R. 1980. The expanding envelope of Zeta Puppis - A detailed UV-line fit. *A&A*, **84**(Apr.), 342–349.

Hamann, W.-R. 1981. Line formation in expanding atmospheres - On the validity of the Sobolev approximation. *A&A*, **93**(Jan.), 353–361.

Hubeny, I., and Mihalas, D. 2014. *Theory of Stellar Atmospheres.*

Hummer, D. G., and Rybicki, G. B. 1971. Radiative transfer in spherically symmetric systems. The conservative grey case. *MNRAS*, **152**, 1.

Hummer, D. G., and Rybicki, G. B. 1985. The Sobolev approximation for line formation with continuous opacity. *ApJ*, **293**(June), 258–267.

Kudritzki, R.-P., and Puls, J. 2000. Winds from Hot Stars. *ARA&A*, **38**, 613–666.

Lamers, H. J. G. L. M., Cerruti-Sola, M., and Perinotto, M. 1987. The 'SEI' method for accurate and efficient calculations of line profiles in spherically symmetric stellar winds. *ApJ*, **314**(Mar.), 726–738.

Lucy, L. B. 1971. The Formation of Resonance Lines in Extended and Expanding Atmospheres. *ApJ*, **163**(Jan.), 95.

Lucy, L. B., and Solomon, P. M. 1970. Mass Loss by Hot Stars. *ApJ*, **159**(Mar.), 879–893.

Mihalas, D. 1978. *Stellar atmospheres (2nd edition).* San Francisco: W. H. Freeman and Co., 1978.

Mihalas, D., Kunasz, P. B., and Hummer, D. G. 1975. Solution of the comoving frame equation of transfer in spherically symmetric flows. I - Computational method for equivalent-two-level-atom source functions. *ApJ*, **202**(Dec.), 465–489.

Mihalas, D., Kunasz, P. B., and Hummer, D. G. 1976. Solution of the Comoving-Frame Equation of Transfer in Spherically Symmetric Flows. III. Effect of Aberration and Advection Terms. *ApJ*, **206**(June), 515–524.

Morton, D. C., and Underhill, A. B. 1977. The ultraviolet spectrum of Zeta Puppis. *ApJS*, **33**(Jan.), 83–99.

Olson, G. L., Auer, L. H., and Buchler, J. R. 1986. A rapidly convergent iterative solution of the non-LTE line radiation transfer problem. *J. Quant. Spec. Radiat. Transf.*, **35**(June), 431–442.

Owocki, S. P., and Puls, J. 1996. Nonlocal Escape-Integral Approximations for the Line Force in Structured Line-driven Stellar Winds. *ApJ*, **462**(May), 894.

Owocki, S. P., and Puls, J. 1999. Line-driven Stellar Winds: The Dynamical Role of Diffuse Radiation Gradients and Limitations to the Sobolev Approach. *ApJ*, **510**(Jan.), 355–368.

Pauldrach, A., Puls, J., and Kudritzki, R. P. 1986. Radiation-driven winds of hot luminous stars - Improvements of the theory and first results. *A&A*, **164**(Aug.), 86–100.

Pauldrach, A. W. A., Hoffmann, T. L., and Lennon, M. 2001. Radiation-driven winds of hot luminous stars. XIII. A description of NLTE line blocking and blanketing towards realistic models for expanding atmospheres. *A&A*, **375**(Aug.), 161–195.

Puls, J. 1987. Radiation-driven winds of hot luminous stars. IV - The influence of multiline effects. *A&A*, **184**(Oct.), 227–248.

Puls, J. 1991. Approximate lambda-operators working at optimum convergence rate. II - Line transfer in expanding atmospheres. *A&A*, **248**(Aug.), 581–589.

Puls, J., and Herrero, A. 1988. Approximate Lambda-Operators working at optimum convergence rate. I - Theory and application to hydrostatic atmospheres. *A&A*, **204**(Oct.), 219–228.

Puls, J., and Hummer, D. G. 1988. The Sobolev approximation for the line force and line source function in a spherically-symmetrical stellar wind with continuum opacity. *A&A*, **191**(Feb.), 87–98.

Puls, J., Owocki, S. P., and Fullerton, A. W. 1993. On the synthesis of resonance lines in dynamical models of structured hot-star winds. *A&A*, **279**(Nov.), 457–476.

Puls, J., Urbaneja, M. A., Venero, R., Repolust, T., Springmann, U., Jokuthy, A., and Mokiem, M. R. 2005. Atmospheric NLTE-models for the spectroscopic analysis of blue stars with winds. II. Line-blanketed models. *A&A*, **435**(May), 669–698.

Puls, J., Vink, J. S., and Najarro, F. 2008. Mass loss from hot massive stars. *A&A Rev.*, **16**(Dec.), 209–325.

Rybicki, G. B., and Hummer, D. G. 1978. A generalization of the Sobolev method for flows with nonlocal radiative coupling. *ApJ*, **219**(Jan.), 654–675.

Rybicki, G. B., and Hummer, D. G. 1991. An accelerated lambda iteration method for multilevel radiative transfer. I - Non-overlapping lines with background continuum. *A&A*, **245**(May), 171–181.

Santolaya-Rey, A. E., Puls, J., and Herrero, A. 1997. Atmospheric NLTE-models for the spectroscopic analysis of luminous blue stars with winds. *A&A*, **323**(July), 488–512.

Simón-Díaz, S., and Stasińska, G. 2008. The ionizing radiation from massive stars and its impact on HII regions: results from modern model atmospheres. *MNRAS*, **389**(Sept.), 1009–1021.

Sobolev, V. V. 1957. The Diffusion of Lα Radiation in Nebulae and Stellar Envelopes. *Soviet Ast.*, **1**(Oct.), 678.

Sobolev, V. V. 1960. *Moving envelopes of stars*. Cambridge: Harvard University Press, 1960.

Taresch, G., Kudritzki, R. P., Hurwitz, M., Bowyer, S., Pauldrach, A. W. A., Puls, J., Butler, K., Lennon, D. J., and Haser, S. M. 1997. Quantitative analysis of the FUV, UV and optical spectrum of the O3 star HD 93129A. *A&A*, **321**(May), 531–548.

Trujillo Bueno, J., and Fabiani Bendicho, P. 1995. A Novel Iterative Scheme for the Very Fast and Accurate Solution of Non-LTE Radiative Transfer Problems. *ApJ*, **455**(Dec.), 646.

Werner, K., and Husfeld, D. 1985. Multi-level non-LTE line formation calculations using approximate Lambda-operators. *A&A*, **148**(July), 417–422.

# Thanks a lot
### for your attention!

# … questions?